**US Army Corps
of Engineers**
Hydrologic Engineering Center

Flow Transitions in Bridge Backwater Analysis

September 1995

RD-42

REPORT DOCUMENTATION PAGE

Form Approved OMB No. 0704-0188

1. AGENCY USE ONLY *(Leave blank)*	2. REPORT DATE September 1995	3. REPORT TYPE AND DATES COVERED Research Document No. 42	

4. TITLE AND SUBTITLE
Flow Transitions in Bridge Backwater Analysis

5. FUNDING NUMBERS

6. AUTHOR(S)
John H. Hunt, Gary W. Brunner

7. PERFORMING ORGANIZATION NAME(S) AND ADDRESS(ES)
US Army Corps of Engineers
Institute for Water Resources
Hydrologic Engineering Center
609 Second Street
Davis, CA 95616-4687

8. PERFORMING ORGANIZATION REPORT NUMBER
RD-42

9. SPONSORING / MONITORING AGENCY NAME(S) AND ADDRESS(ES)
N/A

10. SPONSORING / MONITORING AGENCY REPORT NUMBER
N/A

11. SUPPLEMENTARY NOTES

12a. DISTRIBUTION / AVAILABILITY STATEMENT
Approved for Public Release. Distribution of this document is unlimited.

12b. DISTRIBUTION CODE

13. ABSTRACT *(Maximum 200 words)*

Bridges across floodplains may require special attention in one-dimensional hydraulic modeling if they cause severe contraction and expansion of the flow. The accurate prediction of the energy losses in the contraction reach upstream of the bridge and the expansion reach downstream of the bridge using one-dimensional models presents particular difficulty. Modeling these reaches requires the accurate evaluation of four parameters: the expansion reach length, L_e; the contraction reach length, L_c; the expansion coefficient, C_e; and the contraction coefficient, C_c. This report presents research conducted by the author to investigate these four parameters through the use of field data, two-dimensional hydraulic modeling, and one-dimensional modeling.

14. SUBJECT TERMS
Bridge, Hydraulics, Backwater, Contraction and Expansion, energy losses, HEC-RAS, RMA-2, Steady Flow Analysis

15. NUMBER OF PAGES
81

16. PRICE CODE

17. SECURITY CLASSIFICATION OF REPORT UNCLASSIFIED	18. SECURITY CLASSIFICATION OF THIS PAGE UNCLASSIFIED	19. SECURITY CLASSIFICATION OF ABSTRACT UNCLASSIFIED	20. LIMITATION OF ABSTRACT UNLIMITED

NSN 7540-01-280-5500

Standard Form 298 (Rev. 2-89)
Prescribed by ANSI Std. Z39-18
298-102

Flow Transitions in Bridge Backwater Analysis

September 1995

US Army Corps of Engineers
Institute for Water Resources
Hydrologic Engineering Center
609 Second Street
Davis, CA 95616

(530) 756-1104
(530) 756-8250 FAX
www.hec.usace.army.mil

Table of Contents

Table of Contents

List of Figures

List of Tables

Acknowledgement

Abstract

Bridges across floodplains may require special attention if they cause severe contraction and expansion of the flow. The accurate prediction of the energy losses in the contraction reach upstream of the bridge and the expansion reach downstream of the bridge using one-dimensional models presents particular difficulty. Modeling these reaches requires the accurate evaluation of four parameters: the expansion reach length, L_e; the contraction reach length, L_c; the expansion coefficient, C_e; and the contraction coefficient, C_c. This thesis presents research conducted by the author to investigate these four parameters through the use of field data, two-dimensional hydraulic modeling, and one-dimensional modeling.

Regression equations for evaluating the parameters are reported, as well as more general recommendations regarding the range of values of each parameter. It was concluded from this study that the traditional rule of thumb which recommends the assumption of an expansion rate of one unit outward for every four units downstream overestimates the reach length in most cases. The standard rule of thumb regarding contraction reach lengths, which assumes a one-to-one rate of contraction, was not refuted by this study, but more refined estimates are possible by using the current recommendations. The traditional standard values, recommended in the past for the expansion and contraction coefficients at bridges, were found to be too high in most instances.

Chapter 1

Introduction

1.1   Purpose

Hydraulic studies frequently require an accurate evaluation of the hydraulic impacts of bridges. In bridge design a hydraulic analysis is vital to the proper design of the span length, low chord, abutments, and piers. Hydraulic scour has been responsible for many bridge failures throughout the United States, and many more existing bridges are vulnerable to damage or failure by scour (Federal Highway Administration [FHWA], 1991). Scour prediction usually requires a hydraulic analysis of the river reach containing the bridge. Flood insurance studies in urban areas usually involve one or more bridge structures which must be included in the hydraulic analysis.

Two-dimensional numerical models are increasingly available to hydraulic engineers for use in bridge-related studies. For most practical studies, however, one-dimensional models are preferred, given their relative ease of use and the fact that most riverine systems are approximated reasonably well as one-dimensional systems. The most commonly used one-dimensional models for studies involving bridges are HEC-2 by the Hydrologic Engineering Center of the U.S. Army Corps of Engineers (Hydrologic Engineering Center [HEC], 1990) and WSPRO by the U.S. Geological Survey in cooperation with the Federal Highway Administration (FHWA, 1986). In addition to these two steady-flow models, the unsteady-flow model UNET (HEC, 1995a) is frequently applied to reaches which include bridges. Soon HEC-2 and UNET will be replaced by the HEC-River Analysis System (HEC-RAS).

For one-dimensional analyses, the reach affected by a bridge is subdivided into three parts (Figure 1). The contraction reach upstream from the bridge between Sections 3 and 4; the constricted reach bounded by Sections 2 and 3 on the ends and by the bridge abutments on the sides; and the expansion reach downstream from the bridge, bounded on the ends by Sections 1 and 3. The contraction and expansion reaches (hereafter referred to collectively as the transition reaches) have presented the most uncertainty to modelers. Frequently the transition reaches are responsible for most of the energy loss associated with a bridge. The author, in cooperation with the HEC staff and University of California faculty members, has conducted an investigation of the energy loss at flow transition reaches through bridges.

Specifically, the flow field configuration and energy loss in the transition reaches were investigated. Two-dimensional hydraulic models of actual bridge-constricted stream reaches were created and calibrated. In addition, two-dimensional models of idealized stream and constriction geometries were developed. The two-dimensional model results, along with observed data, were used over a range of hydraulic conditions to develop relationships between key parameters used by HEC one-dimensional models and the geometric conditions of the reach. This report presents the findings of the study and seeks to provide improved guidance to users of one-dimensional models on the proper modeling of these transition reaches.
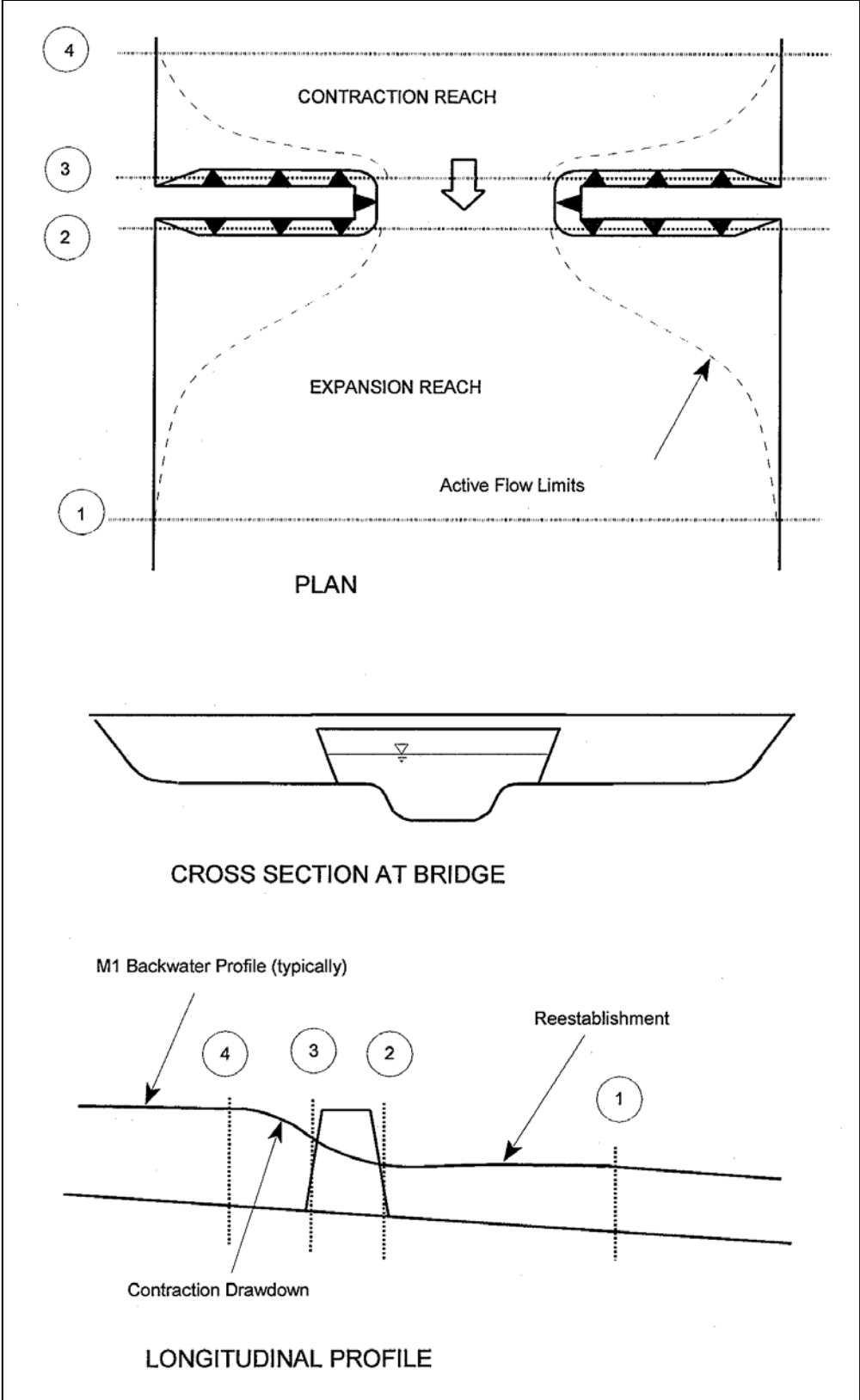
Figure 1 Flow at Bridges: Plan, Section, and Profile

1.2   Bridge Hydraulics Concepts

When the approach embankments of a bridge obstruct the floodplain, energy losses are increased locally, and the result is an increase in the water surface elevation upstream of the bridge for a given discharge. That is, the water surface elevation upstream is higher than it would be if the bridge were not there. This is illustrated by Figure 1.

The nature of flow through constrictions is described by Chow (1959). In subcritical flow, a backwater region is created in which the flow depth is greater than it would be under unconstricted conditions. The location where the backwater effect is greatest is considered to be the upstream end of the contraction reach and is represented by Section 1 on Figure 1. Flow velocity and friction loss increase with distance from this point toward the bridge. Additional energy loss in this reach is due to increased velocities and the turbulent exchange of momentum which accompanies contracting flows.

In the immediate vicinity of the bridge constriction, between Sections 2 and 3 in Figure 1, the water surface dips sharply, and the flow velocity reaches a maximum. The flow here is often considered to be rapidly varied. High energy loss between Sections 2 and 3 is due to the extremely high velocities and the drag exerted by piers and abutments. Downstream from the bridge, between Sections 1 and 2, the flow expands to reestablish full-width flow conditions. This is referred to as the expansion reach. The energy loss is more than normal in this reach due to the higher flow velocities and the turbulent momentum exchange associated with expanding flow.

The expansion reach is typically analyzed as a gradually-varied-flow reach. This is a problematic approximation, given the fact that the depth and velocity in this reach are influenced by upstream conditions, as discussed above, even in subcritical flow. This situation does not meet the conditions assumed in the derivation of the equation for gradually-varied-flow. In both the contraction and expansion reaches, the assumption of one-dimensional flow causes limitations in the accurate modeling of the flow therein. This issue is discussed at length in Chapters 3 and 4 of this report. All of the excess energy loss caused by a bridge occurs between the point of maximum backwater upstream and the point of full expansion downstream (Sections 4 and 1 respectively).

When the flow is subcritical downstream, through, and upstream of the bridge, the hydraulic control is at, or downstream of, Section 1. In some cases, however, the constriction is so great as to force the flow under the bridge to pass through critical depth, and the hydraulic control is at the most constricted section. This study has focused only on fully subcritical scenarios. The concepts described above are particularly applicable to situations in which the flow moves through the constriction without submerging the bridge low chord or overtopping the roadway. This study does not address the special problems of overtopping or pressure flow.

Chapter 2

Literature Review

Much practical research on bridge waterway hydraulics has been carried out in the United States since the early 1950's. The Federal Highway Administration (formerly the Bureau of Public Roads, BPR) has been involved in bridge hydraulics research because of the large federal investment in highway bridges throughout the country. The United States Geological Survey (USGS) has carried out several research projects under contract with the FHWA. Additionally, the USGS often uses water surface measurements at bridge constrictions to compute approximate discharge values. This indirect measurement method has motivated some bridge-related research by USGS. The U.S. Army Corps of Engineers (Corps), in its flood control and floodplain management missions, has also been concerned with the effects of bridges on river hydraulics. The Corps' research efforts in this regard are partially reflected in the river hydraulics computer programs developed by HEC.

2.1   USGS Method of Indirect Discharge Measurement

Often the direct measurement of peak discharge in high flow events is impossible using standard current-meter methods. For these circumstances the USGS has developed an indirect measurement technique which utilizes the measurement of peak water surfaces (usually by high water marks) upstream and downstream from abrupt constrictions. The constrictions are generally those caused by bridges.

Indirect measurement methods were used by the USGS for many years without adequate verification or documentation. Finally, Kindsvater, Carter, and Tracy (USGS, 1953) presented a formal method based on the results of a laboratory research program at the Georgia Institute of Technology. The method is commonly referred to as the "contracted-opening method." The discharge formula in the contracted-opening method expresses the peak discharge as a function of the change in water surface elevation between an upstream section and the most contracted downstream section. The basic form of the discharge equation is

$$Q = CA_2 \sqrt{2g \left(\Delta h + \alpha_4 \frac{V_4^2}{2g} - h_f \right)} \tag{1}$$

in which:

  Q   =   peak discharge in cfs,

  C   =   coefficient of discharge,

A_2 =   gross area of Section 2, in square feet,

g   =   acceleration due to gravity in ft/s^2,

Δh =   difference in water surface elevation between the approach section (Section 4) and the most contracted section inside the bridge, in feet,

h_f =   head loss in feet due to friction between the approach and contracted sections,

α_4 =   kinetic energy correction coefficient at Section 4, and

V_4 =   average velocity at Section 4 in feet per second.

Section 4 is the upstream end of the contraction reach (also referred to as the approach section), and Section 2 is usually taken as the most constricted section (see Figure 1).

With the equation in this form, an iterative solution technique is required to find the discharge since V_4 and h_f are not known in advance. In a paper published later, Tracy and Carter (1955) presented an extension of this method for use in predicting the backwater associated with a given discharge.

In the application of the contracted-opening method, the approach section is generally taken to be located upstream from the constriction a distance equal to the width of the bridge opening. Section 2 is typically located at the downstream end of the constriction. The authors noted that the depth at Section 2 is not only dependent upon downstream conditions but is highly dependent upon the flow conditions within the constriction.

The coefficient C, in Equation 1, is described by the authors as accounting for several factors: the reduction of flow area inside the constricted reach (to a vena contracta); energy loss to eddy production in the contraction reach and the constricted reach; and the non-uniform velocity distribution in Section 2. An extensive series of charts is included in the documentation for the evaluation of C under different conditions. These charts were derived empirically using the data from the Georgia Tech laboratory study. The engineer first obtains a base coefficient CN which is a function of abutment type, degree of channel constriction, and constriction length to width ratio. The value of C is eventually obtained after C' is modified by several factors which are dependent upon the Froude number at Section 2, abutment details, and skew angle to the main flow.

2.2   FHWA Method

In a discussion of the contracted-opening method, Izzard (1955) suggested that a simplified relationship between backwater and a Froude number within the constriction would be sufficiently accurate for bridge design purposes. Izzard acknowledged that the relationship would need to be developed and verified by laboratory and field research. The proposed relationship was

$$\frac{h_4}{h_n} = K\frac{V_n^2}{2gh_n} = K\frac{Fr_n^2}{2} \qquad (2)$$

in which:

h_4 = hydraulic depth at Section 1,

h_n = the unconstricted "normal" depth, i.e. the depth which would occur without the bridge constriction,

K = a coefficient, a function of abutment type, configuration, skew, eccentricity, piers, etc.

V_n = a hypothetical velocity associated with h_n at the constricted section, that is the velocity which would result by dividing the discharge by the gross area in the constricted section below h_n, and

Fr_n = a Froude number at the constricted section associated with h_n and V_n.

The Bureau of Public Roads, under Mr. Izzard's initiative, subsequently conducted a research project (Liu, Bradley, and Plate, 1957) to provide a practical method of analyzing the backwater at bridges. The research was carried out at the facilities of Colorado State University. Approximately 1400 runs were made in tilting flumes. The flume models varied with respect to discharge and slope. Channel shapes included rectangular and compound cross sections. The bridge models simulated various abutment types and configurations. The researchers were concerned primarily with the backwater, h_4^* which is the height of the water surface above the normal water surface for a given discharge. They presented a dimensional analysis which led to the following equation:

$$\frac{h_4^*}{h_n} = f\left[Fr_n,\ \mathrm{Re}_n,\ \frac{B}{h_n},\ \frac{b}{B},\ type\right] \qquad (3)$$

in which:

h_4^* = backwater as described above,

Re_n = Reynolds number associated with the hypothetical velocity V_n in the constriction,

B = top width of unconstricted flow,

b = constriction opening width, and

type = the shape of the abutment.

The Colorado State study resulted in the following equation for backwater (FHWA, 1978):

$$h_4^* = K * \alpha_3 \frac{V_n^2}{2g} + \alpha_4 \left[\left(\frac{A_n}{A_1} \right)^2 - \left(\frac{A_n}{A_4} \right)^2 \right] \frac{V_n^2}{2g} \tag{4}$$

in which:

K^* = the backwater coefficient which is a function of the severity of the constriction, abutment type and shape, piers, eccentricity, and skew,

α_3 = velocity distribution coefficient at Section 3 (see Figure 1),

A_n = the area at the constricted section (taken as Section 3 in this method) below the "normal" water surface, h_n, and

A_1, A_4 = the areas at Sections 1 and 4, respectively.

The value of K^* is determined in a manner similar to the evaluation of C in the contracted-opening method. First a chart is used to obtain the base value, K_b, as a function of the severity of the constriction and the abutment shape. Incremental terms are added to K_b which account for piers, eccentricity, and skew, to arrive at a total which becomes K^*. This method does not use as many adjustment factors for K^* as the contracted-opening method uses for C. The use of this method requires an iterative procedure since A_4 is a function of h_4^*.

The development of this method incorporated some important assumptions. The presence of A_1 in the equation acknowledges the fact in subcritical flow that the control is at Section 1. The authors mentioned the difficulty of determining the length of the expansion reach. They avoided the need to evaluate this length by assuming that the unconstricted reach was uniform in slope, cross section, and flow conditions. This assumption, when incorporated in the energy equation between Sections 1 and 4, allowed the unconstricted energy loss due to friction to cancel with the elevation change due to bed slope. The total energy loss causing backwater, that in excess of the unconstricted energy loss, was then expressed as a function of K^* and the theoretical velocity for Section 3 below normal depth (V_n). The result of this formulation was that all reach lengths were absent in the final equation. A related assumption was that $\alpha_1 = \alpha_4$.

Another key concept in the development and use of this method is the hypothetical properties of the gross area of Section 3 below the "normal" water surface elevation. The property A_n is the area of Section 3 below the level which would be the water surface elevation if the floodplain were not constricted at this location. The velocity V_n is the total discharge divided by A_n.

The location of Section 4, the approach section, was defined as the point of maximum backwater, as in the contracted-opening method. The distance from the bridge embankment to this point was expressed as an empirical function of bridge opening width, the flow depth under the bridge, and the eccentricity of the opening.

8

This method was adopted as the standard for bridge hydraulic analysis in 1960. The backwater coefficient base curves were significantly revised later to agree better with field prototype data obtained in the late 1960's (FHWA, 1978).

2.3   Later USGS Research

Both of the methods described above were developed primarily from laboratory data, with only a limited amount of data available from field sites. When field data became available, both methods were found to be weak in their ability to provide consistently accurate backwater estimates. Beginning in 1969 the USGS, in cooperation with the FHWA and the Mississippi, Alabama, and Louisiana State Highway Departments, undertook a study to collect backwater and discharge data at 20 bridge sites. All of the sites had wide, heavily-vegetated floodplains. The FHWA and USGS methods described above were found to be poorly suited for these conditions. These data were used in the development and verification of a new hydraulic analysis method by Schneider et al. (USGS, 1977) which proved to be more accurate when applied to the field sites that had been studied.

Unlike the contracted-opening method and the FHWA method which lump all of the excess energy losses into a single empirical coefficient, this method divides the total energy loss into three parts: approach reach, constricted reach, and expansion reach. In the approach reach, the energy loss is taken as the average friction slope multiplied by the average streamline length for that reach. A table is provided by the authors, to be used in evaluating the average approach streamline length as a function of the severity of the constriction. This table was derived from a detailed analysis based on two-dimensional horizontal potential flow. The constricted reach losses are similarly computed by multiplying the friction slope for the most contracted section by the straight-line reach length. Total losses between the approach section and the downstream end of the constricted reach (Sections 4 and 2 respectively) are thus computed by the following:

$$h_f(4-2) = Q^2 \left[\frac{L_a(4-3)}{K_4 K_c} + \frac{L(3-2)}{K_2^2} \right] \tag{5}$$

in which:

$h_f(4\text{-}2)$ = total energy loss between Sections 4 and 2,

Q = discharge,

$L_a(4\text{-}3)$ = average streamline length in the approach reach,

K_i = conveyance at Section i, computed by Manning's equation,

K_c = the smaller of the conveyances K_2 and K_q, and

K_q = the portion of the total Section 4 conveyance contained within the bridge width.

The expansion reach losses are subdivided into two components: friction losses and flow expansion losses. The friction losses, similar to those in the other reaches, are evaluated by the average friction slope times the expansion reach length. The authors incorporate the assumption that Section 1 is located one bridge opening width downstream from the bridge in the formula for friction loss in this reach. For flow expansion loss, the authors present, without derivation, an approximate solution of the momentum, energy, and continuity equations for an idealized rectangular channel expansion. The friction loss and flow expansion loss equations are given next.

For friction losses

$$h_f(2-1) = \frac{bQ^2}{K_1 K_c} \tag{6}$$

For flow expansion losses

$$h_e = \frac{Q^2}{2gA_1^2}\left[2(\beta_1 - \alpha_1) - 2\beta_2\frac{A_1}{A_2} + \alpha_2\left(\frac{A_1}{A_2}\right)^2\right] \tag{7}$$

In Equations 6 and 7

h_e = the headloss due to flow expansion,

b = the bridge opening width, and

β_i = the momentum correction coefficient for momentum at Section i

The authors also present an equation for the approximation of α_2 and β_2 as functions of the discharge coefficient C from the contracted opening method. The approximations are presumably made necessary by the constricted flow section within the bridge constriction which would make an analytical evaluation of these coefficients difficult. This method laid the foundation for the development of a water-surface-profile computer program by Shearman et al. (FHWA, 1986). This program, known as WSPRO, incorporates all of the concepts in the above-described method into its numerical algorithms along with additional routines for pressure and overtopping flow. More discussion of WSPRO appears in Section 3.2 of Chapter 3.

2.4   Other Literature

Laursen (1970) described the bridge backwater problem as involving four zones: accretion upstream from the bridge, contraction in the immediate vicinity of the bridge, expansion just downstream, and abstraction farther downstream. These zones make up a continuum rather than a set of distinctly-bounded regions. The contraction and expansion zones are characterized by rapidly-varied flow. A jet is formed within the contraction zone which is diffused through turbulence in the expansion zone. The contraction and expansion of flow in these regions is

10

dominated by turbulent mixing, while the transitions in the accretion and abstraction zones are governed by resistance to flow and the consequent hydraulic gradients.

Laursen proposed an analysis method which incorporates a user-estimated accretion or abstraction rate into the momentum equation. While lending insight into the problem, Laursen's method has thus far been impractical because there is no known way of determining the rates of abstraction and accretion.

Albertson et al. (1950) .studied the diffusion of submerged two-dimensional and three-dimensional jets (from slots and orifices, respectively) into a fluid at rest. All of the experimental measurements were made in air. Particularly significant to the bridge hydraulics problem were the conclusions of the study with regard to the generalized mean flow pattern downstream from slots. The conclusions indicated under the flow conditions of the investigation that the region of active flow expands at a rate of one unit outward on each side for every four units downstream.

The implication for bridge hydraulics was an expansion zone downstream of a bridge that should be modeled as growing at a rate of four units downstream to one outward. As will be discussed later in this report, the four on one expansion concept has been widely taught as a rule of thumb for modeling bridge expansion reaches. One argument against the direct transfer of the results of Albertson et al. to the bridge problem is that boundary resistance was not significant in their study and that there was no free surface effect. Bridge waterway hydraulics, in contrast, is greatly influenced by the bed and banks of the floodplain downstream and by the presence of a free surface. In a very smooth flume at the University of California (DeVries, 1995), the flow was found to expand at a rate of four on one downstream from a constriction in width.

Recognizing the two-dimensionality of flow at bridges and the difficulty this poses in one-dimensional analysis, several investigators have proposed the application of two-dimensional mathematical models to bridge problems. Franques and Yannitell (1974) developed a two-dimensional finite element model which computes the locations of streamlines through the flow field and then computes energy losses by Bernoulli's equation along the streamlines. Tseng (FHWA, 1975) proposed a finite element model which solves the depth-integrated form of the Reynolds equations to obtain the velocity in two directions at each node along with the depth.

Both of the finite element models mentioned above were applied in simulating the hydraulics of an observed high-flow event at Tallahalla Creek, Mississippi. Both models, with calibration of the resistance parameters, accurately reproduced the longitudinal water surface profile and the transverse variations in water surface throughout the region of interest. Thompson and James (1988) applied the FHWA model FESWMS, a finite-element model which solves the depth-integrated Reynolds equations, to an observed event at Buckhorn Creek, Alabama, with good results in comparison with the observed data.

These results show that two-dimensional finite-element models can be used to model many bridge hydraulics problems successfully. The greater expense, however, in terms of the modeler's time, knowledge, and computer resources, is currently an inhibiting factor in the use of two-dimensional models. It is reasonable to expect that in the near future one-dimensional models will remain the tool of choice for most practical bridge hydraulics studies. It should also

be remembered that depth-integrated two-dimensional models are themselves approximations of the actual dynamics in any flow field.

2.5 HEC Computer Programs

The Hydrologic Engineering Center developed and has maintained for years the computer program HEC-2, a steady-flow one-dimensional model which computes river water surface profiles and includes the capability of modeling the flow through bridges (HEC, 1990). Currently HEC is developing the eventual replacement for HEC-2, known as River Analysis System or HEC-RAS (HEC, 1995b and c). The HEC-RAS bridge modeling techniques are discussed in more detail in section 3.1 of Chapter 3.

Chapter 3

One-Dimensional Modeling

In modern practice the hydraulics of waterways at bridges is analyzed by using mathematical simulation models. The simulation models incorporate site-specific and event-specific data supplied by the engineer into approximate solutions of the governing equations. The computer programs most commonly used in the United States are those developed by HEC and the WSPRO program from the FHWA. The HEC programs and WSPRO utilize the one-dimensional conservation equations -- continuity, conservation of energy, and conservation of momentum -- to compute water surface profiles in stream reaches. The methods employed by these two programs are described in this chapter.

3.1   HEC Model: HEC-RAS

Bridge hydraulics modeling is an important component of the river hydraulics programs developed by HEC. The computer program HEC-RAS is HEC's latest hydraulic simulation program and is the most advanced with respect to bridge hydraulics. The steady-flow, one-dimensional conservation equations are solved by HEC-RAS in the following forms:

Conservation of Mass:

$$Q_u = Q_d \tag{8}$$

and

$$V_u A_u = V_d A_d \tag{9}$$

Conservation of Energy:

$$WS_u + \frac{\alpha_u V_u^2}{2g} = WS_d + \frac{\alpha_d V_d^2}{2g} + h_L \tag{10}$$

with

$$h_L = L \, \bar{S}_f + C \left| \frac{\alpha_u V_u^2}{2g} - \frac{\alpha_d V_d^2}{2g} \right| \tag{11}$$

Conservation of Momentum:

$$\frac{\beta_u Q^2}{gA_u} + \bar{y}_u A_u = \frac{\beta_d Q^2}{gA_d} + \bar{y}_d A_d + \frac{F_{ext}}{\rho g} + \frac{F_w}{\rho g} + \frac{F_a}{\rho g} \qquad (12)$$

in which:

Q $\quad=\quad$ discharge,

V $\quad=\quad$ average flow velocity = Q/A,

A $\quad=\quad$ flow area,

WS $=\quad$ water surface,

α $\quad=\quad$ velocity distribution coefficient for energy,

β $\quad=\quad$ velocity distribution coefficient for momentum,

g $\quad=\quad$ acceleration of gravity,

L $\quad=\quad$ reach length between the upstream section and downstream section,

$\bar{S}_f$ $\quad=\quad$ average friction slope, computed using Manning's equation,

C $\quad=\quad$ transition loss coefficient,

$\bar{y}$ $\quad=\quad$ depth from water surface to center of gravity of flow section,

F_{ext} $=\quad$ sum of streamwise components of external forces exerted on water by flow boundary, such as bed and bank friction or drag from piers,

F_w $\quad=\quad$ streamwise component of weight of water between upstream and downstream sections,

F_a $\quad=\quad$ streamwise component of force due to the difference in flow area between the upstream and downstream sections (neglected in HEC-RAS), and

ρ $\quad=\quad$ density of fluid.

The subscripts u and d denote upstream and downstream sections, respectively.

The computational methods of HEC-RAS are described in detail in the HEC-RAS Hydraulic Reference Manual (HEC, 1995c). As described earlier, the bridge region can be divided into three zones: the contraction reach between Sections 4 and 3; the constricted reach between Sections 3 and 2; and the expansion reach between Sections 2 and 1. The change in water

surface elevation in the constricted reach can be computed using either the energy equation or the momentum equation, depending on the user's preference. In the case of flow passing through critical depth at the constriction (referred to as class B flow), the momentum equation is used to determine the downstream extent of supercritical flow by identifying the approximate location at which a hydraulic jump must occur.

This study has focused exclusively on the contraction and expansion or transition reaches. In these reaches the standard step method (Chow, 1959) is used to balance the energy between the two end sections. This is an iterative scheme which utilizes the continuity and energy equations (Equations 9, 10, and 11). Successful modeling of the hydraulics at a bridge depends largely upon the proper modeling of the transition reaches. Figure 2 is a conceptual illustration of the transition reaches as modeled by HEC-RAS.
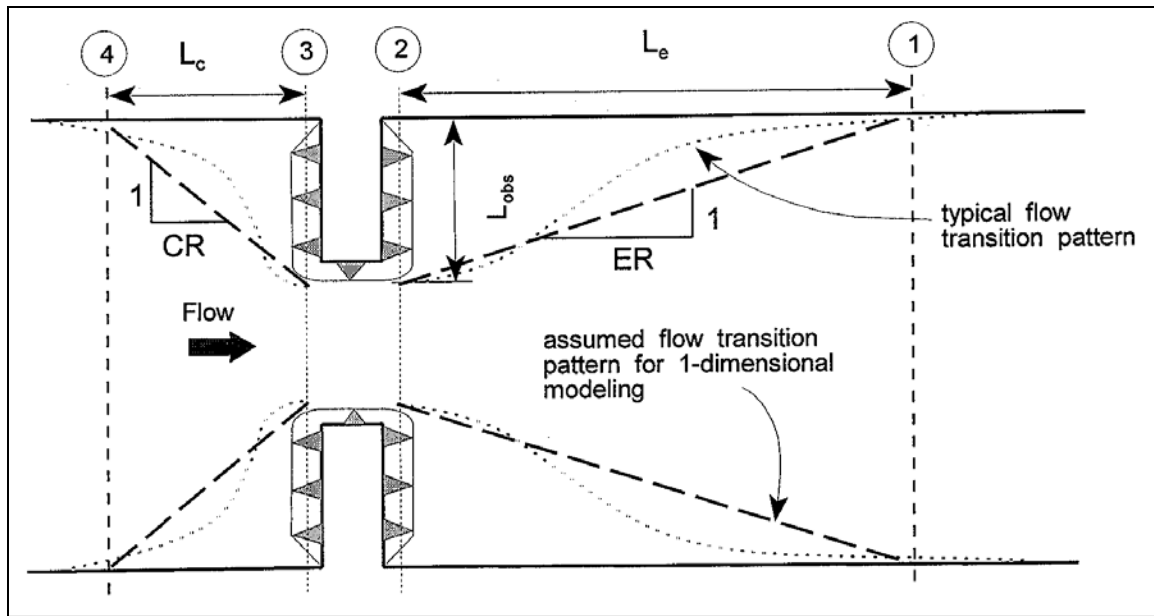
Figure 2 Conceptual Illustration of Transition Reaches.

At Sections 2 and 3 the effective flow width is limited to approximately the width of the bridge opening. This causes increased mean flow velocities at these sections and thus an increase in the value of $\overline{S}_f$ for both transition reaches. The first right-hand term in Equation 11, which represents friction loss, is therefore increased. Since there is often a large difference between the velocity heads of the end sections of the transition reaches, the remainder of Equation 11, which represents transition losses due to turbulent mixing, is more significant in these reaches than in normal reaches.

It can therefore be seen that both components of the energy loss, as expressed in Equation 11, are expected to be greater in the transition reaches than in normal reaches. Accurate determination of the energy losses in the transition reaches requires the user to supply the proper values for four key parameters: the contraction and expansion reach lengths (L_c and L_e respectively) and the coefficients of contraction and expansion (C_c and C_e). The reach lengths are multiplied by their respective friction slopes to obtain friction losses, and the coefficients are multiplied by the absolute difference in velocity head between the two ends of each reach to

obtain the transition loss. Traditionally, flow-width transitions are modeled as being linear
tapers between the ends of the reaches, as shown in Figure 2. The standard approach has been to
use an expansion ratio of 4:1 and a contraction ratio of 1:1 in the absence of site-specific field
observations. The expansion ratio and contraction ratio (ER and CR, respectively in Figure 2)
are defined as the lengths of the transition reaches divided by half of the total reduction in the
width of the original section. The dimension L_{obs} in Figure 2 is the floodplain obstruction length
of one of the bridge approach embankments. Half of the total reduction in the width of the
original section can be expressed as L_{obs} in the case of a symmetric constriction or as $\overline{L}_{obs}$, the
average obstruction length, in the case of an asymmetric constriction.

To date, little conclusive guidance has been available regarding the values of L_c, L_e, C_c, and
C_e. The primary purpose of this study was to relate these four parameters to hydraulic and
geometric variables which the model user can easily evaluate. The relationships obtained appear
in Chapter 7, and it is intended that they will be used to provide improved guidance to the users
of one-dimensional hydraulic models.

3.2   FHWA Model: WSPRO

The emphasis of this study has been on improving the practical use of the various HEC river
hydraulics programs, in particular HEC-RAS. This discussion of the WSPRO methodology
(FHWA, 1986) is presented to highlight the similarities and differences between it and the HEC
methods. Users of the WSPRO program may also benefit from the information provided in this
report.

The equations which form the basis of WSPRO's modeling of bridges were presented in
Section 2.3 of Chapter 2. Like the HEC-RAS program, the problem is conceptually broken into
three reaches. Also like HEC-RAS, friction losses evaluated by Manning's equation play an
important role in the analysis. With respect to the transition reaches, however, two important
differences stand out.

The first difference is the use of a special expansion loss equation by WSPRO (Equation 7).
This equation is reportedly derived by combining approximations of the continuity, energy, and
momentum equations between Sections 1 and 2 (USGS, 1977). The literature does not present
this derivation. During the course of this study, the authors who presented the equation were
contacted, but they did not provide support for it. Attempts at deriving the formula by the
research team for this study led to the conclusion that the development of the equation requires
several important approximations. One apparent approximation is that the downstream reach
geometry is rectangular and prismatic. Also the depth at Section 2 is assumed to be equal to the
depth at Section 1. Once these approximations are made, the resulting equation (Larock, 1995)
is:

$$h_e = \frac{Q^2}{2gA_1^2}\left[(4\beta_1 - \alpha_1) - 4\beta_2 \frac{A_1}{A_2} + \alpha_2\left(\frac{A_1}{A_2}\right)^2\right] \tag{13}$$

Obviously, this equation is different from Equation 7 used by WSPRO. As mentioned in Section 2.3 of Chapter 2, the coefficients α_2 and β_2 are related by the authors to the contraction coefficient of the contracted-opening-method, but the literature does not present derivations for these relationships. Given the lack of support for either the expansion loss equation or the formula for the velocity distribution coefficients, it was concluded that the expansion equation may not be valid and should not be utilized in any HEC methodology. While the WSPRO program does not restrict the user with regard to the chosen expansion reach length to be used in determining friction losses, the users' manual seems to recommend a reach length equal to one bridge opening width, as opposed to HEC's recommendations of relating the expansion distance to the obstruction width.

The other major difference between WSPRO and HEC-RAS is in WSPRO's use of the "effective flow length" concept. The WSPRO method does not compute separate contraction losses in the contraction reach. Instead the developers contend that the friction loss alone is an adequate estimate of total energy loss in the contraction reach, provided that a conveyance-weighted average reach length is used. This average length, termed the effective flow length, is computed in the program by dividing the contraction reach into twenty stream tubes of equal conveyance, computing the length of each tube, and taking the arithmetic average of the tube lengths as the effective flow length. According to the authors, the approach section may always be placed at the location one bridge-opening width upstream from the bridge, and the effective flow length method will cause the correct total energy loss to be computed for the contraction reach.

When the HEC programs are used at bridges, the main channel and overbank reach lengths that are used should acknowledge the transitioning nature of the streamlines. For example, the overbank reach lengths in an otherwise straight floodplain should be longer than the main channel lengths in the transition reaches where the streamlines are not parallel. It could be said then that the HEC models provide for a user-controlled version of the effective flow length concept, since the overall reach length used by HEC models in balancing reach energy is the conveyance-weighted length of the two overbanks and the main channel.

3.3   Verification of One-Dimensional Models using Field Data

As part of this research project, a study was conducted to compare the computed water surface results from HEC-RAS, HEC-2, and WSPRO with the observed water surfaces for seventeen different flood events at 13 different field sites containing bridges. The data for each event and site included the measured peak discharge, high water marks throughout the reach, and the measured transverse velocity distribution at the bridge opening. The data was compiled into Hydrologic Investigations Atlases by Arcement, Colson, and Ming (USGS, 1978 and 1979). With reasonable calibration of the parameters of Manning's n value, the transition reach lengths, and the transition coefficients, all three programs performed well. Errors in the predicted water surface elevation at the approach section (location of maximum backwater) averaged around three percent of the depth for all of the programs.

One weakness of this study was that all of the field sites were similar in their hydraulic characteristics, with wide and heavily vegetated floodplains, bed slopes from 0.05% to 0.15%

(2.5 feet/mile to 8 feet/mile), and generally low excess energy loss caused by the bridge. The simulation and comparison results for all of the events are recorded in a Hydrologic Engineering Center study report (HEC, 1995d).

Table 1 shows the average absolute error in the water surface elevations based on a comparison of three locations at each bridge site. The three locations of interest were just downstream of the bridge (Section 2), at the approach section (Section 4), and at the next cross section upstream of the approach section. The average absolute error at each site and event was computed by taking the sum of the absolute values of the differences between the observed and computed water surfaces at the three locations, and dividing this sum by three. The mean of the average absolute error values was 0.24 for HEC-RAS, 0.26 for HEC-2, and 0.33 for WSPRO. While these results indicated that HEC-RAS performed better than the other two programs, the differences in performance are not sufficient to conclude that any of the three is superior.

Table 1
Verification and Comparison of One-Dimensional Hydraulics Programs

Study Location	Q cfs	Average Absolute Error, feet		
		HEC-RAS	HEC-2	WSPRO
Alexander Creek, Alabama	5500	0.20	0.30	0.17
Alexander Creek, Alabama	9500	0.10	0.13	0.23
Beaver Creek, Louisiana	14000	0.07	0.03	0.50
Bogue Chitto, Mississippi	25000	0.23	0.27	0.23
Bogue Chitto, Mississippi	31500	0.40	0.27	0.33
Buckhorn Creek, Alabama	4150	0.20	0.20	0.23
Cypress Creek, Louisiana	1500	0.23	0.30	0.17
Flagon Bayou, Louisiana	4730	0.27	0.30	0.30
Okatama Creek near Magee, Mississippi	16100	0.17	0.20	0.23
Okatama Creek east of Magee, Mississippi	12100	0.40	0.47	0.80
Pea Creek, Alabama	1780	0.37	0.37	0.50
Poley Creek, Alabama	1900	0.30	0.37	0.40
Poley Creek, Alabama	4600	0.20	0.23	0.50
Tenmile Creek, Louisiana	6400	0.23	0.23	0.10
Thompson Creek, Mississippi	3800	0.20	0.20	0.40
Yellow River, Alabama	2000	0.17	0.17	0.23
Yellow River, Alabama	6600	0.40	0.30	0.43

One important observation from this exercise in the use of the HEC methods was that the standard approach of using a 4:1 ratio to determine the expansion reach length consistently caused an over prediction of energy loss in the expansion reach. This finding supported the need for further study of transition reach configurations. For these sites the expansion reach length which consistently gave the best results was approximately one bridge-opening width. Since the method used by WSPRO was itself designed to fit these same field data (USGS, 1977), it is not surprising that the user documentation for the program implies that the expansion reach length should be equal to one bridge-opening width.

Chapter 4

Two-Dimensional Hydrodynamic Modeling

In certain situations the complexity of the flow field in the vicinity of the bridge makes the application of a one-dimensional model questionable. When a bridge has multiple openings, for instance, a one-dimensional model may be inadequate. In such cases a two-dimensional model may be required. This chapter describes the advantages of two-dimensional models, the governing equations typically used, and the input parameters required.

4.1   Advantages of Two-Dimensional Models

When a one-dimensional model is used in any river hydraulics problem, the water surface is assumed to be level across any cross section perpendicular to the main flow direction. In some important situations, including flood flows in the vicinity of bridges, the level-water-surface assumption is incorrect. Water surfaces can be superelevated, convex or concave along a cross-section line. One advantage of two-dimensional models is that they allow the simulation of such transverse variations in water surface elevation. As an example, in most two-dimensional models developed in this study, the model outputs consistently indicated a concave transverse water surface just upstream of the bridge, a convex transverse surface just downstream, and a highly-varied transverse surface within the constricted reach due to the piers.

Another major advantage of two-dimensional analyses in bridge hydraulics is in the handling of flow contraction and expansion. Chapter 3 describes the principles of the one-dimensional modeling of flow through bridges. A significant degree of uncertainty lies in the one-dimensional representation of the transition reaches. The user must somehow estimate the length of each transition reach and also estimate the values of the constants which will be multiplied by the difference in velocity heads at the ends of each transition reach.

In essence these estimations are the attempt to approximate the two-dimensional aspects of the flow field. The reach length approximation effort and the incorporation of transition loss coefficients are an acknowledgment that much of the energy available in the transition reaches goes into the lateral movement of water and the exchange of momentum via turbulence. The available energy, therefore, cannot be fully utilized for the downstream movement of water. A two-dimensional analysis is able to simulate the lateral redistribution and turbulent momentum exchange in these reaches. This capability eliminates the need for the estimation of transition reach lengths and transition loss coefficients. A two-dimensional analysis does, however, have some input uncertainties of its own, which are discussed in Section 4.3 of this chapter.

4.2   Governing Equations

The two-dimensional modeling for this study was done using the program RMA-2 (King, 1994) developed by Resource Management Associates (RMA). This program is a finite element model which utilizes the depth-averaged Reynolds equations (also known as the shallow water equations) to determine the x-velocity component and y-velocity component as well as the depth at each node in a horizontally-defined network. The equations solved by RMA-2 can be expressed as follows:

The continuity equation:

$$\frac{\partial h}{\partial t} + \frac{\partial (uh)}{\partial x} + \frac{\partial (vh)}{\partial y} = 0 \tag{14}$$

The momentum equations:

$$\frac{\partial u}{\partial t} + u\frac{\partial u}{\partial x} + v\frac{\partial u}{\partial y} + g\left(\frac{\partial h}{\partial x} + \frac{\partial a}{\partial x}\right) - \frac{\varepsilon_{xx}}{\rho}\frac{\partial^2 u}{\partial x^2} - \frac{\varepsilon_{xy}}{\rho}\frac{\partial^2 u}{\partial y^2} + \frac{gu}{C^2 h}\sqrt{u^2 + v^2} = 0 \tag{15}$$

$$\frac{\partial v}{\partial t} + u\frac{\partial v}{\partial x} + v\frac{\partial v}{\partial y} + g\left(\frac{\partial h}{\partial y} + \frac{\partial a}{\partial y}\right) - \frac{\varepsilon_{yx}}{\rho}\frac{\partial^2 v}{\partial x^2} - \frac{\varepsilon_{yy}}{\rho}\frac{\partial^2 v}{\partial y^2} + \frac{gv}{C^2 h}\sqrt{u^2 + v^2} = 0 \tag{16}$$

In these equations

a   =   bottom elevation at a node,

h   =   flow depth at a node,

t   =   time,

x   =   distance in the x-direction,

y   =   distance in the y-direction,

u   =   depth-averaged horizontal flow velocity in the x-direction,

v   =   depth-averaged horizontal flow velocity in the y-direction,

g   =   acceleration due to gravity,

ρ =   water density,

ε_{xx} =   normal eddy viscosity coefficient in the x-direction,

ε_{xy} =   transverse eddy viscosity coefficient in the x-direction,

ε_{yx} = transverse eddy viscosity coefficient in the y-direction,

ε_{yy} = normal eddy viscosity coefficient in the y-direction, and

C = Chezy roughness coefficient (converted from Manning's n coefficient if the latter is entered by the user).

These equations must be solved for each node at each time step. The solution is accomplished in RMA-2 by a finite element technique. The description of finite element techniques is beyond the scope of this report but can be found in two reports produced by RMA (Norton et al., 1973 and King, 1993). All of the two-dimensional simulations in this study were steady-state, meaning that all time derivative terms were zero.

4.3   Input Parameters

As with one-dimensional models, a primary input requirement for RMA-2 is the description of the geometry of the floodplain. In one-dimensional modeling the geometric description consists of a series of cross sections taken perpendicular to the main flow direction, related to one another by reach lengths. Hydraulic structures such as bridges require a description via input data of piers, abutments, etc. either as cross-sectional components or as structure-specific items. The geometric input to RMA-2 requires an accurate three-dimensional representation of the locations and orientations of the major geometric features such as main channels, overbank lines, swales, and obstructions. This representation is in the form of a bathymetric model which describes the variation of the bed level throughout the entire horizontal extent of the system being modeled.

In addition to the bathymetric model, the system geometry is defined by the computational mesh. This mesh usually is created by the modeler with the use of a graphical data preprocessor. The mesh consists of elements and nodes. Elements are triangular or quadrilateral shapes with nodes at the corners and midsides. Nodes are points at which the numerical values of the independent variables (velocities and depth) will be computed numerically. The elements can be highly irregular in size and shape, although regular shapes are preferred. The computational accuracy and stability of the RMA-2 model depends to a large extent upon the size and regularity of the elements. In general smaller elements lead to a higher mesh density and greater accuracy and stability for the model. The advantage of high mesh density, however, must be weighed against the fact that computation time increases with mesh density. A desirable mesh density is one that is just adequate for stability and the required accuracy. Two-dimensional models of bridge-constricted reaches should have a high mesh density within the constriction and the immediate vicinity of the bridge, with the density gradually decreasing with distance from the bridge.

Bed and bank friction forces are modeled using the Chezy coefficient. If the user enters Manning's n instead of the Chezy coefficient in the input data, the n value is converted to an equivalent Chezy coefficient. Each element is given a type number. Bed and bank roughness coefficient values are contained in the definition of each element type.

In the momentum equations (15 and 16), the terms involving the second partial derivatives of the velocity represent turbulent transport. Each eddy viscosity or turbulent exchange coefficient is supplied by the user and determines the magnitude of these terms in the equations. As with the roughness coefficients, the eddy viscosity coefficients are included in the definition of each element type. In addition to modeling turbulence, the turbulence terms damp numerical oscillations, so that higher values of ε generally lead to greater stability in the solution scheme.

To select the value of this coefficient for maximum simulation accuracy requires knowledge of the transverse velocity distributions in the prototype flow field for various flow conditions. Since this information is not usually known, the proper evaluation of the eddy viscosity coefficients can be difficult. One potential error in the application of RMA-2 is the overestimation of the eddy viscosity. An excessively high value might provide a very stable solution, but the resulting velocity and depth values could be inaccurate. This outcome can occur because excessive numerical damping can cause key features of the prototype flow field, such as separation zones or sharp velocity gradients, to be missed. When no data regarding prototype velocity distributions is available, the general rule within the Corps of Engineers is to keep eddy viscosity coefficients as low as possible without introducing stability problems.

When one-dimensional and two-dimensional hydraulic models are created for the same prototype, there will usually be a difference in the calibrated Manning's n values between the two models. In one-dimensional models, the resistance associated with turbulent fluctuations is lumped into the roughness coefficient. In two-dimensional models the turbulence resistance is computed separately from the bed and bank friction resistance. For this reason the roughness coefficients in the two-dimensional model should be somewhat less than those in the one-dimensional model.

Chapter 5

Analysis of Transition Reach Lengths

This study began as an exercise to verify the performance of the one-dimensional programs HEC-2, WSPRO, and HEC-RAS using field data. This verification effort is described in Section 3.3 of Chapter 3. One significant finding from that study was that the use of the traditional 4:1 expansion rate criterion consistently led to over prediction of the energy loss in the expansion reach. That is, the expansion reach length determined by this method was too long. It was this finding that most indicated the need for further study of the transition reach lengths.

The two-dimensional hydrodynamics program RMA-2 was utilized extensively to study the transition reach lengths. The two-dimensional modeling effort consisted of two phases. First, several of the flood events at the actual field sites were modeled. Then, once the adequate performance of the program was established, two-dimensional models of a large number of idealized floodplain and bridge geometries were studied.

5.1   Two-Dimensional Models of Field Sites

The first phase of the two-dimensional modeling had two purposes. The first was to test the ability of the model to simulate accurately the water surface longitudinal profile and transverse variations corresponding to each flood event. The second was to gain insight into the lengths and configurations of the transition reaches for the situations modeled.

Five flood events at three different sites were modeled. The bathymetric models were created by digitizing the endpoints of the given cross sections from paper maps, and putting this data along with the cross section coordinates into the land surface modeling software SURFER (Golden Software, 1994). A surface model file produced in SURFER was reformatted as an RMA-2 map file which enabled the transfer of the bathymetric data to a computational grid. The number of elements in the computational meshes (including both quadrilateral and triangular elements) ranged from about 850 to about 1100. Each element was assigned a type number. The definition of each type number included the values of the Manning n coefficients and the eddy viscosity coefficients. The eddy viscosity coefficient values were calibrated, by successive trial and error and adjustment of the values in each element type definition, to reproduce the velocity distribution which was measured at the face of each bridge. The Manning's coefficients were calibrated in the same manner as the eddy viscosity coefficients to match the measured high-water marks in the downstream region of each site, on the assumption that the far downstream regions were not affected by the bridge constriction.

After calibration in the manner described, the output water surface contours from the two-dimensional models were compared with the observed high water marks. For four of the models, the maximum difference between the computed and observed water surface elevations at a point was less than or equal to 0.5 feet, and the typical differences were less than 0.3 feet. These

models were as follows: Buckhorn Creek, Q = 4150 cfs and Q = 2250 cfs; Okatama Creek, Q = 16100 cfs; and Poley Creek, Q = 1900 cfs. The fifth model, Poley Creek, Q = 4600 cfs showed a maximum error of about one foot on the downstream side of the bridge but agreed much better with the data on the upstream side. The water surface contours in the RMA-2 outputs generally reflected the transverse water surface variations suggested by the high water marks.

Since the water surface elevation data are high-water marks left on trees after the flood had passed, the value at any point could easily be in error by 0.2 feet or more. Given the potential for error in the observed data and the limitations in accurate bathymetric modeling of the sites, it was judged that the RMA-2 program had performed well in simulating these flood events. Figure 3(a) is a plot of the water surface elevation contours computed by RMA-2 for one of the events at Buckhorn Creek. Figure 3(b) shows water surface elevation contours near the bridge for the same event, along with the values and locations of some observed water surface elevations. Tables 2(a) through (e) present the computed versus observed water surface elevation for each cross section at each site. At cross sections where the water surface elevation varies considerably, the elevations reported are those in the vicinity of the main channel.
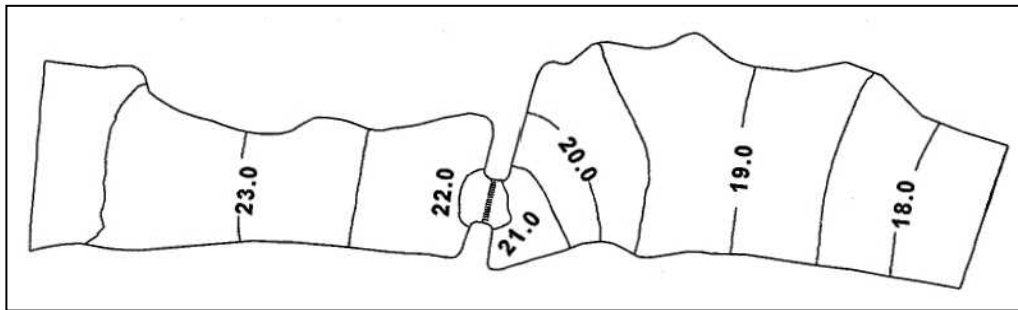
Figure 3(a) Buckhorn Creek, Q = 4150 cfs. Water Surface Contours from RMA-2.
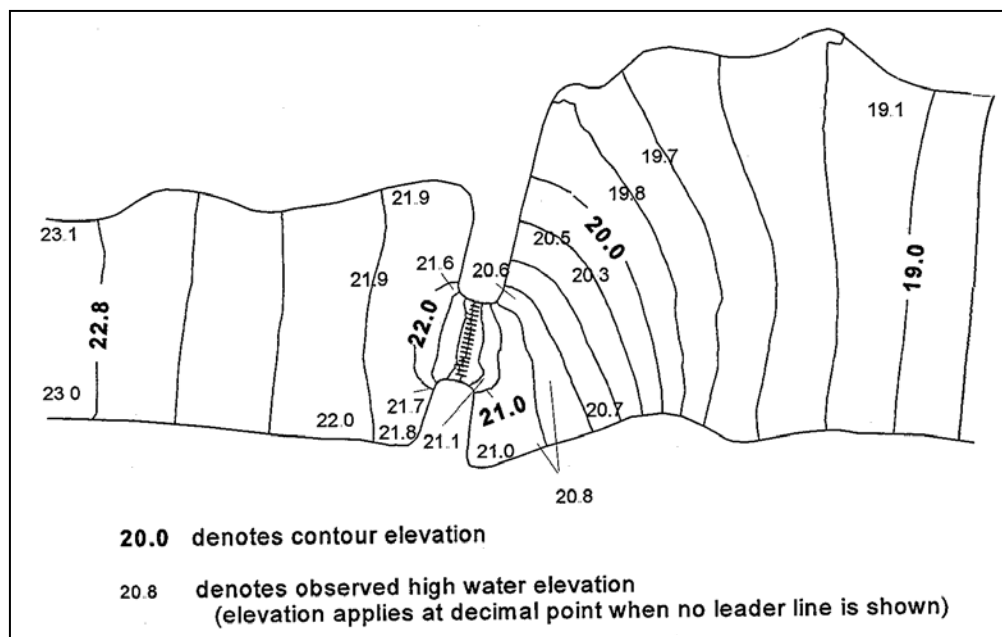
Figure 3(b) Buckhorn Creek, Q = 4150 cfs. Water Surface Contours from RMA-2 with Observed High Water Mark Elevations.

Table 2(a)
Buckhorn Creek, Q = 4150 cfs, Water Surface Elevations
Observed and Computed by RMA-2

Section Number from Hydrologic Atlas	Distance from Arbitrary Reference Pt. (feet)	Water Surface Elevation (feet)		Error (feet)
		Observed	Computed by RMA-2	
2	1030	17.5	17.5	0.0
3	2340	19.0	19.0	0.0
4	3030	20.0	19.7	-0.3
5	3380	20.5	20.5	0.0
5 1 Br. Dnstrm.	3710	20.8	21.1	0.3
5.4 Br. Upstrm.	3750	21.6	21.9	0.3
6	4940	21.9	22.1	0.2
7	4990	23.1	22.9	-0.2

Table 2(b)
Buckhorn Creek, Q = 2250 cfs, Water Surface Elevations
Observed and Computed by RMA-2

Section Number from Hydrologic Atlas	Distance from Arbitrary Reference Pt. (feet)	Water Surface Elevation (feet)		Error (feet)
		Observed	Computed by RMA-2	
2	1030	15.7	15.7	0.0
3	2340	17.3	17.3	0.0
4	3030	18.4	18.2	-0.2
5	3380	18.9	18.9	0.0
5.1 Br. Dnstrm.	3710	Not Available	19.4	-----
5.4 Br. Upstrm.	3750	Not Available	19.9	-----
6	4940	20.0	20.2	0.2
7	4990	21.0	20.9	-0.1

Table 2(c)
Poley Creek, Q = 4600 cfs, Water Surface Elevations
Observed and Computed by RMA-2

Section Number from Hydrologic Atlas	Distance from Arbitrary Reference Pt. (feet)	Water Surface Elevation (feet)		Error (feet)
		Observed	Computed by RMA-2	
2	1120	33.3	33.2	-0.1
3	1650	34.4	34.1	-0.3
4	1980	34.9	35.1	0.2
4.1 Br. Dnstrm.	2190	35.3	35.8	0.5
4.4 Br. Upstrm.	2220	37.0	36.9	-0.1
5	2480	37.2	37.5	0.3
6	3500	38.0	38.1	0.1

Table 2(d)
Poley Creek, Q = 1900 cfs, Water Surface Elevations
Observed and Computed by RMA-2

Section Number from Hydrologic Atlas	Distance from Arbitrary Reference Pt. (feet)	Water Surface Elevation (feet)		Error (feet)
		Observed	Computed by RMA-2	
2	1120	31.2	31.1	-0.1
3	1650	32.3	32.1	-0.2
4	1980	32.9	33.1	0.2
4.1 Br. Dnstrm.	2190	33.2	33.6	0.4
4.4 Br. Upstrm.	2220	34.6	34.3	-0.3
5	2480	34.8	34.7	-0.1
6	3500	35.6	35.3	-0.3

Table 2(e)
Okatama Creek, Q = 16100 cfs, Water Surface Elevations
Observed and Computed by RMA-2

Section Number from Hydrologic Atlas	Distance from Arbitrary Reference Pt. (feet)	Water Surface Elevation (feet)		Error (feet)
		Observed	Computed by RMA-2	
3	5600	60.0	60.2	0.2
4	7290	62.8	63.0	0.2
5	8060	63.7	63.5	-0.2
6	8580	63.8	63.7	-0.1
6.1 Br. Dnstrm.	8800	63.8	64.0	0.2
6.4 Br. Upstrm.	8840	Not Available	66.1	----
7	9060	67.2	66.9	-0.3
8	9700	67.4	67.4	0.0
9	11100	67.8	67.7	-0.1

The output velocity vector plots from the RMA-2 models were examined so that the lengths of the transition reaches could be estimated. On each velocity vector plot, a line was subjectively drawn across the floodplain, both upstream and downstream of the bridge opening, at the locations that were judged to separate the zones of significant lateral flow from the zones of predominantly streamwise flow. The contraction and expansion ratios were then determined by dividing the distance from each drawn line to the bridge face by the average obstruction length (the sum of obstruction lengths of both approach embankments, divided by two). None of the contraction ratios computed in this manner exceeded 0.7:1 and none of the expansion ratios exceeded 1.4:1. Figure 4 is a velocity vector plot from RMA-2 for one of these models.

6.0 fps
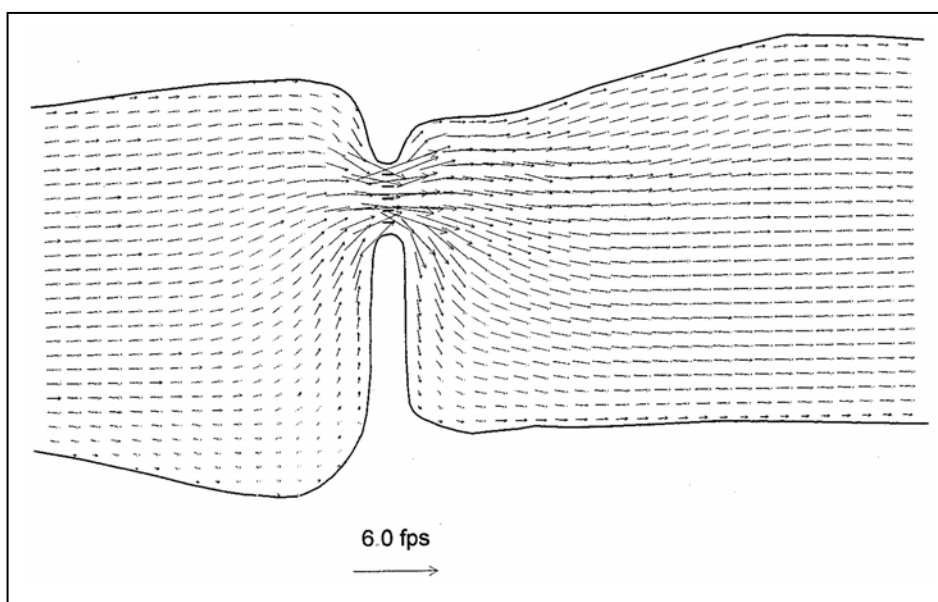
Figure 4 Poley Creek Alabama, Q = 4600 cfs. Velocity Vectors from RMA-2.

5.2   Idealized Two-Dimensional Models

The field prototypes modeled with the one-dimensional and two-dimensional programs had certain hydraulic characteristics in common. All had wide, heavily vegetated overbanks, with Manning's n values from 0.07 to 0.24, and slopes between 2.5 feet/mile and 8.0 feet/mile. An announcement was placed in the HEC newsletter, which has a worldwide distribution in the water resources engineering community, requesting data similar to this USGS data, but for different types of bridge sites. While there were some responses to the request, the data available were not suitable. There are many bridge locations where high water marks have been measured in the vicinity of bridges after high flow events, but very rarely is the peak discharge associated with these high water marks known with adequate accuracy at the bridge location.

5.2.1   Geometry and Input Parameters

To extend the scope and general applicability of the study, it was decided to create a large number of two-dimensional models of idealized floodplain and bridge geometries. Figure 5 shows a typical cross section for the idealized cases. The overall floodplain width was constant at 1000 feet. The main channel n value was constant at 0.04. The other pertinent parameters were systematically varied as follows:

Bridge opening width, b	100, 250, and 500 feet
Discharge, Q	5000, 10000, 20000, and 30000 cfs
Overbank Manning coef., n_{ob}	0.04, 0.08, and 0.16
Bed slope, S	1, 5, and 10 feet/mile
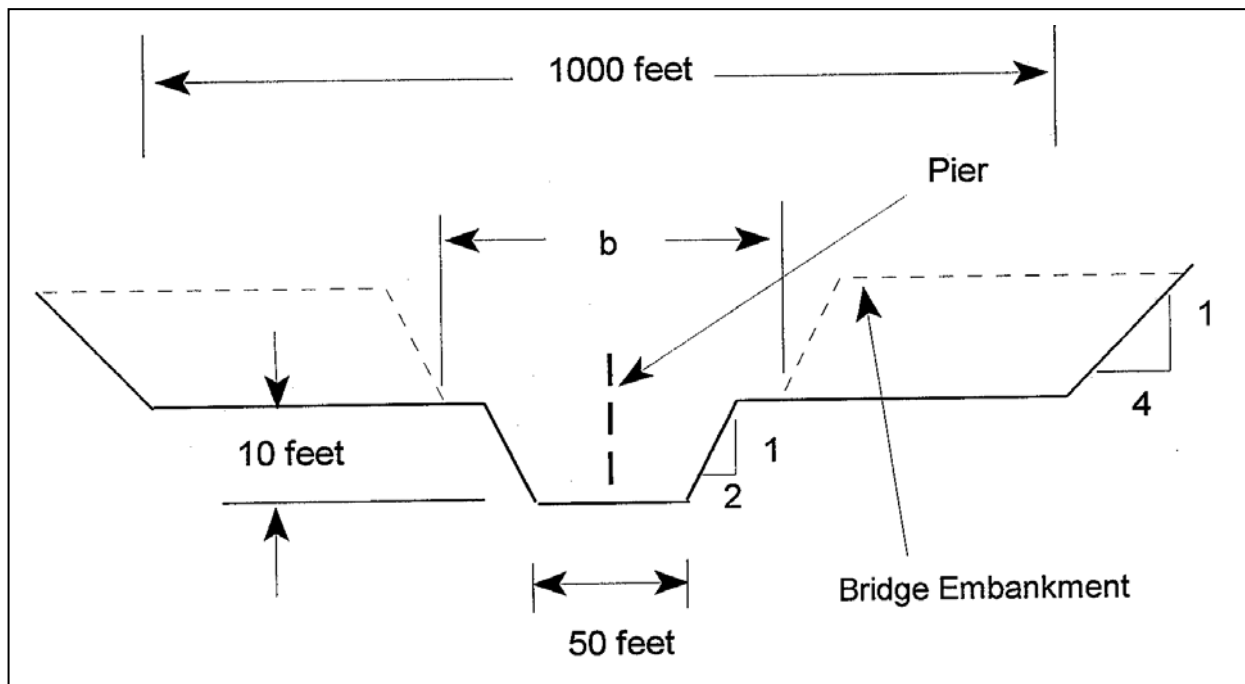
Figure 5 Idealized Case – Cross Section.

In addition to the systematic variation of these parameters, eleven additional cases were created which had vertical abutments rather than spill-through abutments, six cases were developed which had asymmetric rather than symmetric bridge obstructions, and four more cases were studied which were enlarged-scale and reduced-scale versions of four of the standard cases. A total of 97 idealized models were created. Figure 6 illustrates the difference between spill-through and vertical abutments. The asymmetric cases all had spill-through abutments and a bridge opening width of 375 feet with one edge of the opening located 125 feet from the
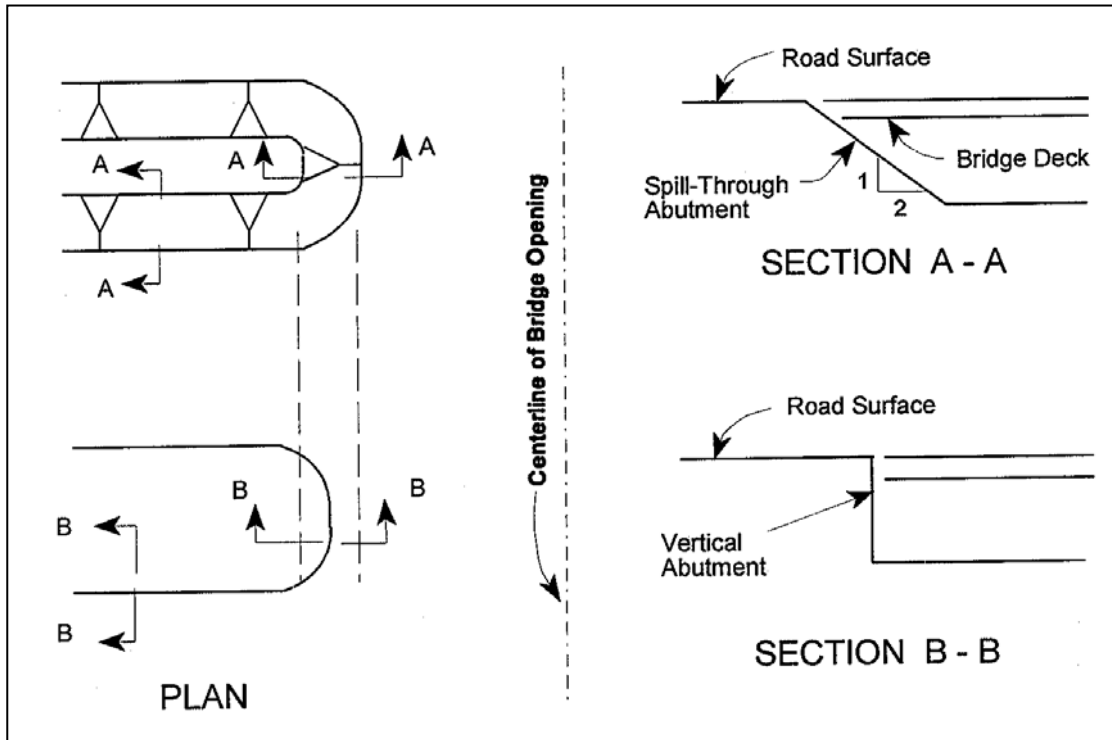
Figure 6 Illustration of Spill-Through and Vertical Abutments.

floodplain centerline. All of the cases included bridge piers which were diamond-shaped in plan with a maximum width of 5 feet. The narrow-opening cases each had one pier. The medium-opening cases each had five piers with 50 foot spacing. Each of the wide-opening cases had nine piers with 50 foot spacing. The pier sets were centered in the bridge opening for all cases.

The density of the finite element network was standard for all cases in a bridge-opening-width class. The elements in the vicinity of the bridge openings were smallest, with a maximum dimension of approximately 15 feet. The largest elements, in the overbanks and far from the bridge, had a maximum dimension of approximately 800 feet. The element count ranged from 900 to 1150 in these idealized models. Figure 7 shows the mesh configuration in the vicinity of the bridge for the medium-opening-width cases with spill-through abutments.

Care was taken to ensure that the network accurately and completely depicted the geometry of the floodplain and bridge components in each model. In each case with spill-through abutments, for instance, the mesh included two rows of quadrilateral elements placed along the sloped faces of the abutments and bridge embankments, and the bottom elevations assigned to the nodes in these elements reflected the 2:1 side slopes. To create a network for a case with vertical abutments, the mesh for the corresponding spill-through case was modified by

29
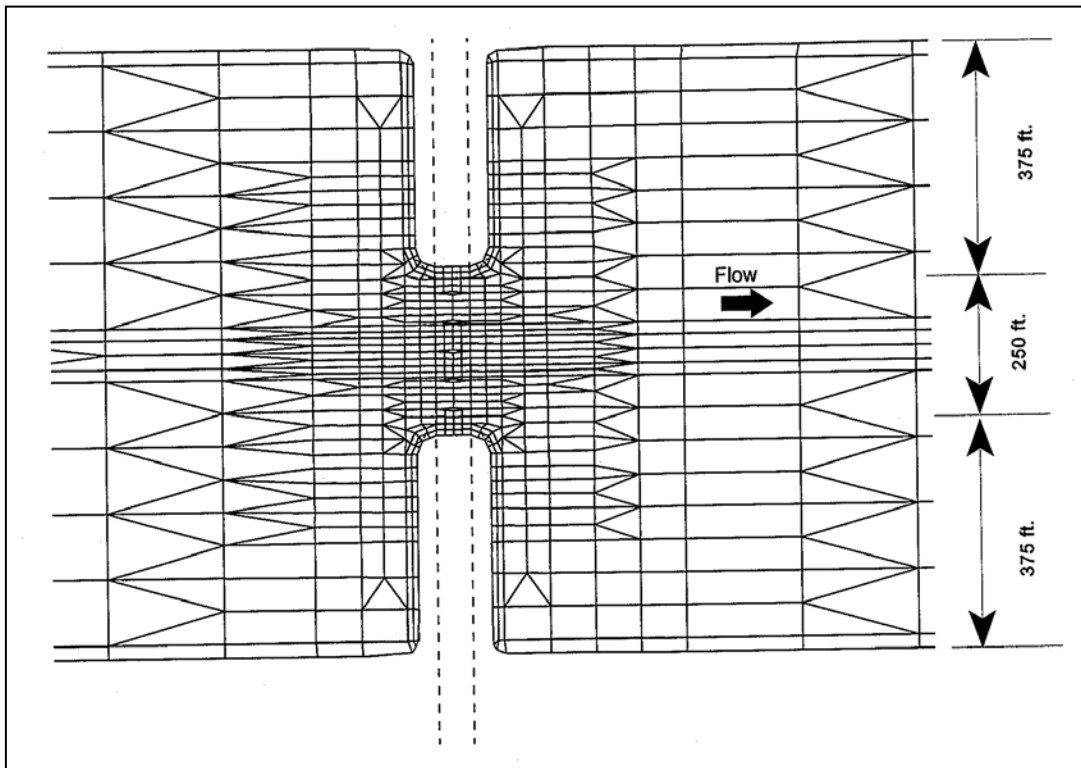
Figure 7 Part of the Finite Element Grid for RMA-2 Idealized Models (Medium-Opening Case Shown).

eliminating the outermost of the two rows of elements along the embankment and abutment slopes. The bottom elevations on the new outer edge were then lowered to eliminate the sloped bank effect. In the computations, RMA-2 treats the distance between the water surface and bottom elevation at any boundary node as a vertical bank with friction.

Aside from the bathymetry and the network configuration, the other major input issue for the idealized RMA-2 models was the evaluation of the eddy viscosity coefficients. Obviously, no calibration data was available. Therefore, the values of the coefficients were generally set as low as possible without creating instability in the model solution.

The RMA-2 program allows the specification of eddy viscosity coefficients by entering a multiplier which the program uses to compute automatically a value for each element based on the maximum dimension of the element. For the idealized cases in this study, the models were given two element types, one for the overbank elements and one for the main channel elements. The value of the multiplier was typically set to 1.0 for both element types originally. Once the model was running and stable for the appropriate boundary conditions, the multipliers would be lowered together gradually, usually to a standard value of 0.25 for all elements.

The standard multiplier value of 0.25 was used to facilitate the execution of such a large number of models in a limited period of time. This value was near the lower limit for all of the cases. The exceptions to the standard value occurred for those models which required slightly higher values to attain convergence. These were typically the cases with the highest velocity gradients in the vicinity of the bridge opening. The actual computed values of the normal eddy viscosity coefficients for the models using the standard 0.25 multiplier value ranged from

30

3.8 lb-sec/ft^2 for the smallest elements (those inside the bridge constriction) to about 200 lb-sec/ft^2 for the largest elements (overbank elements far from the bridge). The actual values of the transverse coefficients were typically less than the normal coefficients. The magnitude of each transverse coefficient was dependent upon the width or smaller dimension of the element to which it was assigned.

5.2.2   Recording of Results

As models were completed, output information was recorded for later use. The output values of interest were the expansion and contraction reach lengths (L_e and L_c respectively) and the water surface elevations at strategic locations in the flow field.

The evaluation of the transition reach lengths for each model proved to be technically challenging. Several methods were tried for defining the downstream end of flow expansion and the upstream end of contraction. The RMA-2 program allows the user to define strings of nodes in a flow field across which the total discharge is computed. The first method attempted for reach length definition was based on the percentage of total discharge conveyed in the overbanks. The overbank discharge percentage was recorded far downstream from the bridge where the flow could reasonably be assumed to be uniform and one dimensional. Then the overbank flow percentage was read for each continuity string progressing upstream until the reduction in the value (as a percentage of total discharge) reached a predetermined magnitude (reductions equal to both 10% and 20% of total discharge were tried), at which point the downstream end of the expansion reach was set. Likewise for the upstream side, the one-dimensional overbank discharge percentage was determined, and then a standard reduced value was located in the contracting region.

The overbank-discharge-percentage method had the advantage of being objective and quantitative in nature. The method was rejected, however, for two reasons. First, when the locations for transition limits determined by this method were superimposed on velocity vector plots, there was a visual inconsistency. Some results fell in regions where the vector plots indicated the flow was very nearly one-dimensional, while others fell in locations on the plots which had significant lateral velocity components. As a second reason for rejection of this method, there was a concern that the values defined in this way might be biased. It was apparent in those cases with a lower normal overbank percentage that a greater deviation from one-dimensional conditions would always be required to cause a reduction equal to 10% of the total discharge in comparison with other flows which had a higher overbank percentage.

Another method that was attempted was based on the examination of velocity contour plots from the RMA-2 results. These plots invariably showed a uniform velocity distribution throughout a long reach at the downstream end of each model, with a sharp inflection of the outer overbank velocity contour at a point that was presumed to be near the downstream limit of the expansion reach. Upstream from this inflection point, the overbank velocity contours showed a streamwise velocity gradient. The gradient indicated that the overbank flow was still developing in this region. A similar pattern occurred in the transition zone upstream of the bridge. This method showed promise but was rejected because the resulting reach limit locations were highly sensitive to the contour interval that was plotted, i.e., a 0.1 feet/sec interval versus

31

0.2 feet/sec. Additionally, the results showed the same inconsistency as the overbank-discharge-percentage method with respect to their superposition on velocity vector plots.

The method which was finally adopted in defining the end of the expansion reach required the examination of the velocity vector plots by two members of the research team. Each of the two evaluators inspected the velocity vector plot for each model and subjectively drew lines across the floodplain where the limits of the expansion and contraction reaches appeared to be. The value that was finally selected was the average of these two estimates.

All of the velocity vector plots had one of two characteristics which aided in these determinations. For those models with significant eddy zones, the point on the flow boundary where the dividing streamline reattached was relatively easy to identify on the plots. The limit of the expansion reach was usually judged to be a short distance downstream from this point. For those models with no significant eddy zones, the flowpaths suggested by the velocity vectors showed strong inflections. Beyond these inflections the streamwise component of velocity dominated. The limits of the transition reaches were usually judged to be a short distance downstream or upstream (for expansion or contraction, respectively) of the zone where these inflections occurred.

The limit of expansion was never taken so far downstream as to be in the region of purely one-dimensional, uniform flow. For the purposes of one-dimensional modeling, in which the active flow width is assumed to expand in a linear fashion from Section 2 to Section 1 (refer to Figure 2), to place the downstream expansion so far downstream would cause an unacceptable over-estimation of the energy losses downstream of the bridge.

The maximum difference in estimations between the two evaluators was 250 feet, but the average difference was approximately 100 feet. Figure 8 is a typical velocity vector plot with the expansion reach limit shown, as defined by this method. This level of accuracy proved to be adequate for the expansion reach lengths, but it was inadequate for the contraction reach lengths.
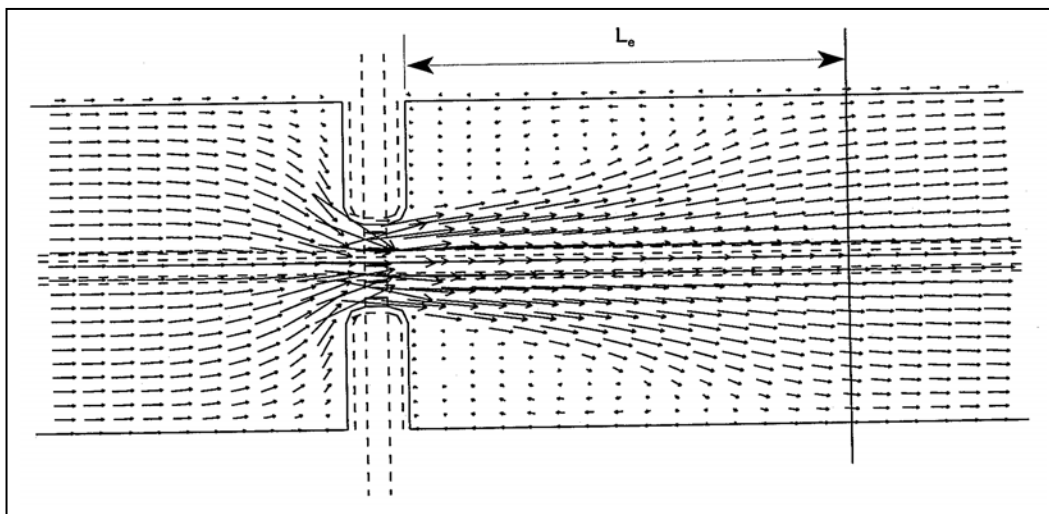
Figure 8   Typical Velocity Vector Plot for Idealized RMA-2 Model with Expansion
Reach Limit Shown.

32

The contraction reach lengths had a range of only about 400 feet compared to 1300 feet for the expansion reach lengths. The variation in the results obtained by using the velocity vector plot method was large relative compared to the range of the contraction reach lengths. This large variation in the results caused the expected trends in the contraction reach length, in relation to the varied hydraulic conditions, to be obscured. It was decided that a completely objective method must be found to define the contraction reach length.

The method that was selected is based on plots of the water surface contours from the RMA-2 output. Water surface contours were plotted at an interval of 0.01 feet. Invariably the contours just upstream of the bridge showed a concave curvature. At any transverse cross section in this region, the minimum water surface elevation occurred at the point which was directly upstream from the center of the bridge opening. On every symmetrical model there was one contour which intersected the flow boundary on both sides near the corner formed by the outer edge of the floodplain and the upstream edge of the bridge embankment. The transverse cross section for which this contour represented the minimum water surface elevation was taken to be the upstream end of the contraction reach.

This definition was based on the assumption that the centerline water surface elevation at the upstream end of the contraction reach is essentially the same as that at the corner formed by the edge of the floodplain and the upstream edge of the bridge embankment (Liu, Bradley, and Plate, 1957). The contraction reach lengths, as defined by this water-surface-contour-based method, showed definite trends related to the varying conditions. Figure 9 shows a typical water surface contour plot and shows the contraction reach limit defined by this method.
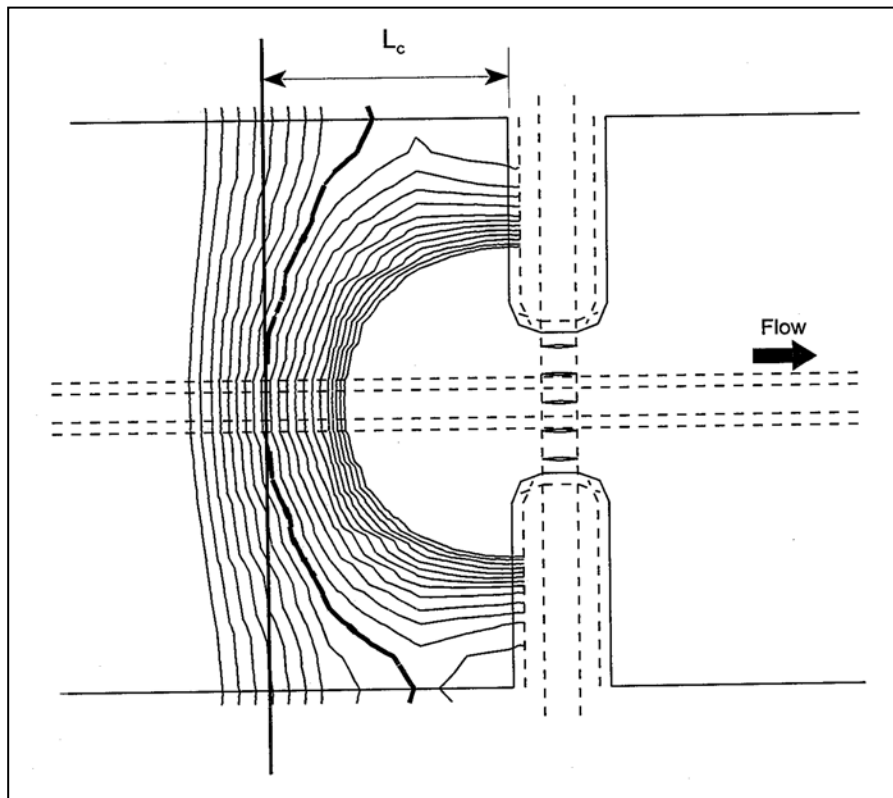
Figure 9 Illustration of Contraction Reach Limit Definition.

Chapter 6

Analysis of Contraction and Expansion
Loss Coefficients

6.1 Calibration of HEC-RAS Models

Once the transition reach lengths were recorded, water surface profile information was taken from the results of each RMA-2 simulation. Using the water surface contour plots again, the water surface elevation was read from the plot for several points on each model, including points far downstream of the bridge, the downstream limit of the expansion reach (Section 1), just downstream of the bridge (Section 2), just upstream of the bridge (Section 3), the upstream limit of the contraction reach (Section 4), and at least one point upstream of Section 1(refer to Figure 1). Where there was curvature in the contour lines, the elevation value taken at each location was that corresponding to the main channel flow (the centerline). Just downstream of the bridge, where the contours frequently indicated standing waves on the water surface over a limited area, the water surface elevation was taken as the arithmetic average of the peak and trough values.

Once the water surface profile results were extracted from the RMA-2 output, the one-dimensional program HEC-RAS was employed to analyze the energy losses in the transition reaches. An HEC-RAS model was made to correspond with each idealized RMA-2 model. Manning's n values were calibrated to match the RMA-2 water surface elevations far downstream of the bridge. The upstream end of the contraction reach and the downstream end of the expansion reach, as taken from the two-dimensional model results, were entered into the one-dimensional models as Sections 4 and 1 respectively. The bridge geometry was entered using the HEC-RAS bridge data editor to correspond with that in the RMA-2 models.

In the one-dimensional models the expansion and contraction coefficients, C_e and C_c respectively, were calibrated to produce the water surface profile which most closely matched the RMA-2 results. The minimum acceptable value for either coefficient was taken to be 0.10, and the calibration was also constrained to prevent the expansion coefficient from ever being smaller than the contraction coefficient. These constraints were introduced in an attempt to avoid results which would be contrary to engineering judgment.

6.2 Expansion Coefficients

In all of the one-dimensional models the depth computed by HEC-RAS for the Section 4 location was the normal depth for that particular slope and roughness. The results from many of the RMA-2 models, however, indicated a smaller depth at this location, even though each one had the same downstream boundary conditions as the corresponding HEC-RAS model. This is a consequence of the fact that the expansion limit was never taken to be so far downstream that the

35

flow was uniform and purely one-dimensional. Whenever the discrepancy between the RMA-2 flow depth and the normal flow depth at this section was less than or equal to 0.3 feet, the HEC-RAS water surface at that location was forced to the average of the RMA-2 and normal depth values. Whenever the discrepancy exceeded 0.3 feet, the expansion limit location was reevaluated, i.e. moved farther downstream until the depth difference was less than or equal to 0.3 feet. This situation occurred in only eight of the cases.

The value of the expansion coefficient C_e was dependent on the target water surface elevation at the section just downstream of the bridge. Where possible, the value of C_e was chosen to produce an exact match between the HEC-RAS and RMA-2 water surface elevation values at this section (to 0.1 foot tolerance). In some cases the differences in velocity heads between Sections 1 and 2 were so small that the coefficient value had no significant effect on the results. In such cases the expansion value was usually given a standard value of 0.30. Another type of special case in the calibration of C_e values is discussed in Section 6.3 of this chapter.

6.3   Contraction Coefficients

The C_c value was adjusted to produce the best possible match between the HEC-RAS and RMA-2 water surface elevations at the upstream end of the contraction reach. This location is also known as the point of maximum backwater or Section 4. This section is the most important one in terms of flood stage prediction. Similarly to the expansion coefficient, in several cases the velocity head difference was too small for the contraction coefficient to affect the results. In these cases the coefficient was set to a standard value of 0.10.

In a few cases the HEC-RAS water surface was slightly higher than the RMA-2 water surface at Section 4, even with a C_c value of 0.10. When this occurred, the possibility of improving the situation by lowering the expansion coefficient value (and thus the Section 2 water surface) was investigated. The expansion coefficient was lowered only when there was a lower value that was possible for the Section 2 water surface elevation than that originally taken from the results. As an example, when the water surface contours at this location in the two-dimensional model indicated standing waves, the trough elevation was the minimum acceptable elevation for the HEC-RAS water surface at Section 2.

In 28 of the HEC-RAS simulations the RMA-2 water surface at Section 4 was at least 0.2 feet lower than could be attained with the HEC-RAS model even if the C_c values were zero. The cases for which this problem appears are the medium-slope and steep-slope cases in the medium-opening and wide-opening classes. There are two possible reasons for this unfortunate situation. One possibility is that the one-dimensional gradually-varied-flow energy loss computation is consistently over predicting the energy loss in this zone of high velocity gradients and rapid change in friction slope. The other possibility is that the RMA-2 models may be underestimating the energy losses within the bridge constriction.

Investigation of the RMA-2 model output files indicated that the volume rate of flow was not completely conserved from one cross section to the next within the constricted zone. As an example, one of the RMA-2 model cases for which this situation exists computed a discharge at the upstream face of the bridge that was only 92.8% of the total upstream discharge. The altered

discharge in the constricted region could mean that the momentum calculations do not consider properly the entire discharge and thus underestimate the velocities and, consequently, the energy lost. Most of the RMA-2 models show similar continuity results in the bridge vicinity. A study of a more refined model, with improved continuity performance, is described in Section 8.5 of Chapter 8. The problem of incomplete conservation of the volume rate of flow in finite element models is discussed by Gray (1980) and Walters and Cheng (1980).

Chapter 7

Results

7.1   General Results

Table 3, parts (a), (b), and (c), lists the input data and the values of the four parameters of interest for each standard-scale symmetric case. The case naming convention used in these tables is as follows:

first character	floodplain width	"m"	denotes medium (1000 feet),
second character	opening width	"w"	denotes wide (500 feet),
		"m"	denotes medium (250 feet),
		"n"	denotes narrow (100 feet),
third character	slope	"f"	denotes flat (1 foot/mile),
		"m"	denotes medium (5 feet/mile),
		"s"	denotes steep (10 feet/mile),
fourth character	abutment type	"v"	if present denotes vertical abutment, absence of "v" denotes spill-through,
numerals	discharge divided by 1000		
last character	overbank roughness	"a"	denotes $n_{ob} = 0.16$,
		"b"	denotes $n_{ob} = 0.04$,
		"c"	denotes $n_{ob} = 0.08$.

In all three parts of Table 3, Q is the discharge, b is the bridge opening width, S is the slope, n_{ob} is the overbank Manning n value, L_c is the contraction reach length, CR is the contraction ratio (the contraction reach length divided by the average obstruction length), C_c is the contraction coefficient, L_e is the expansion reach length, ER is the expansion ratio, and C_e is the expansion coefficient.

Once the data were collected by the methods described in Chapters 5 and 6, they were analyzed with the aid of the statistical analysis program STATGRAPHICS (STSC, 1991). The goals of the statistical analysis were to compile summary statistics and develop regression relationships for the parameters of interest where possible. Table 4 lists the summary statistics for the four parameters.

Table 3(a)
Record of Data for Wide-Bridge-Opening Cases

Case	Q (cfs)	b (feet)	S (ft/mile)	n_{ob}	Contraction			Expansion		
					L_c (feet)	CR	C_c	L_e (feet)	ER	C_e
mwf30a	30,000	500	1	0.16	335	1.34:1	0.10	335	1.34:1	0.30
mwf30b	30,000	500	1	0.04	585	2.34:1	0.10	625	2.50:1	0.30
mwf30c	30,000	500	1	0.08	435	1.74:1	0.10	485	1.94:1	0.20
mwf10a	10,000	500	1	0.16	310	1.24:1	0.10	310	1.24:1	0.30
mwf10b	10,000	500	1	0.04	410	1.64:1	0.10	423	1.69:1	0.30
mwf10c	10,000	500	1	0.08	360	1.44:1	0.10	338	1.35:1	0.30
mwf5a	5,000	500	1	0.16	285	1.14:1	0.10	290	1.16:1	0.30
mwf5b	5,000	500	1	0.04	385	1.54:1	0.10	348	1.39:1	0.10
mwf5c	5,000	500	1	0.08	310	1.24:1	0.10	325	1.30:1	0.30
mwfv30b	30,000	500	1	0.04	560	2.24:1	0.10	645	2.58:1	0.20
mwm30a	30,000	500	5	0.16	295	1.18:1	0.10	308	1.23:1	0.40
mwm30b	30,000	500	5	0.04	485	1.94:1	0.10	523	2.09:1	0.10
mwm30c	30,000	500	5	0.08	375	1.50:1	0.10	405	1.62:1	0.20
mwm10a	10,000	500	5	0.16	275	1.10:1	0.10	260	1.04:1	0.20
mwm10b	10,000	500	5	0.04	360	1.44:1	0.10	370	1.48:1	0.10
mwm10c	10,000	500	5	0.08	310	1.24:1	0.10	335	1.34:1	0.10
mwm5a	5,000	500	5	0.16	300	1.20:1	0.10	260	1.04:1	0.10
mwm5b	5,000	500	5	0.04	315	1.26:1	0.10	323	1.29:1	0.10
mwm5c	5,000	500	5	0.08	295	1.18:1	0.10	298	1.19:1	0.10
mwmv10a	10,000	500	5	0.16	275	1.10:1	0.10	310	1.24:1	0.10
mwmv30a	30,000	500	5	0.16	310	1.24:1	0.10	265	1.06:1	0.40
mws30a	30,000	500	10	0.16	295	1.18:1	0.10	343	1.37:1	0.30
mws30b	30,000	500	10	0.04	485	1.94:1	0.10	510	2.04:1	0.15
mws30c	30,000	500	10	0.08	360	1.44:1	0.10	385	1.54:1	0.50
mws20a	20,000	500	10	0.16	285	1.14:1	0.10	348	1.39:1	0.40
mws20b	20,000	500	10	0.04	410	1.64:1	0.10	468	1.87:1	0.27
mws20c	20,000	500	10	0.08	310	1.24:1	0.10	370	1.48:1	0.30
mws10a	10,000	500	10	0.16	285	1.14:1	0.10	320	1.28:1	0.10
mws10b	10,000	500	10	0.04	335	1.34:1	0.10	345	1.38:1	0.30
mws10c	10,000	500	10	0.08	285	1.14:1	0.10	320	1.28:1	0.25
mwsv30a	30,000	500	10	0.16	295	1.18:1	0.10	335	1.34:1	0.50

Table 3(b)
Record of Data for Medium-Bridge-Opening Cases

Case	Q (cfs)	b (feet)	S (ft/mile)	n_{ob}	Contraction L_c (feet)	CR	C_c	Expansion L_e (feet)	ER	C_e
mmf30a	30,000	250	1	0.16	385	1.03:1	0.10	548	1.46:1	0.40
mmf30b	30,000	250	1	0.04	635	1.69:1	0.10	1110	2.96:1	0.22
mmf30c	30,000	250	1	0.08	495	1.32:1	0.10	760	2.03:1	0.40
mmf10a	10,000	250	1	0.16	335	0.89:1	0.10	635	1.69:1	0.30
mmf10b	10,000	250	1	0.04	510	1.36:1	0.10	660	1.76:1	0.45
mmf10c	10,000	250	1	0.08	395	1.05:1	0.10	510	1.36:1	0.40
mmf5a	5,000	250	1	0.16	335	0.89:1	0.10	460	1.23:1	0.30
mmf5b	5,000	250	1	0.04	460	1.23:1	0.10	585	1.56:1	0.30
mmf5c	5,000	250	1	0.08	360	0.96:1	0.10	510	1.36:1	0.30
mmfv30b	30,000	250	1	0.04	635	1.69:1	0.10	1098	2.93:1	0.38
mmm30a	30,000	250	5	0.16	355	0.95:1	0.10	485	1.29:1	0.60
mmm30b	30,000	250	5	0.04	615	1.64:1	0.30	935	2.49:1	0.35
mmm30c	30,000	250	5	0.08	445	1.19:1	0.10	660	1.76:1	0.45
mmm10a	10,000	250	5	0.16	310	0.83:1	0.10	548	1.46:1	0.10
mmm10b	10,000	250	5	0.04	460	1.23:1	0.10	560	1.49:1	0.25
mmm10c	10,000	250	5	0.08	365	0.97:1	0.10	560	1.49:1	0.10
mmm5a	5,000	250	5	0.16	335	0.89:1	0.10	473	1.26:1	0.10
mmm5b	5,000	250	5	0.04	360	0.96:1	0.10	560	1.49:1	0.10
mmm5c	5,000	250	5	0.08	335	0.89:1	0.10	485	1.29:1	0.10
mmmv30a	30,000	250	5	0.16	360	0.96:1	0.10	485	1.29:1	0.60
mmmv10a	10,000	250	5	0.16	310	0.83:1	0.10	548	1.46:1	0.10
mms30a	30,000	250	10	0.16	335	0.89:1	0.10	735	1.96:1	0.38
mms30c	30,000	250	10	0.08	435	1.16:1	0.10	610	1.63:1	0.50
mms20a	20,000	250	10	0.16	335	0.89:1	0.10	735	1.96:1	0.15
mms20b	20,000	250	10	0.04	535	1.43:1	0.10	673	1.79:1	0.30
mms20c	20,000	250	10	0.08	395	1.05:1	0.10	585	1.56:1	0.38
mms10a	10,000	250	10	0.16	310	0.83:1	0.10	560	1.49:1	0.10
mms10b	10,000	250	10	0.04	410	1.09:1	0.10	660	1.76:1	0.20
mms10c	10,000	250	10	0.08	335	0.89:1	0.10	535	1.43:1	0.10
mmsv30a	30,000	250	10	0.16	335	0.89:1	0.10	735	1.96:1	0.40

Table 3(c)
Record of Data for Narrow-Bridge-Opening Cases

Case	Q (cfs)	b (feet)	S (ft/mile)	n_{ob}	Contraction L_c (feet)	CR	C_c	Expansion L_e (feet)	ER	C_e
mnf30a	30,000	100	1	0.16	385	0.86:1	0.50	9351	2.08:1	0.60
mnf30b	30,000	100	1	0.04	655	1.46:1	0.10	1600	3.56:1	0.55
mnf30c	30,000	100	1	0.08	485	1.08:1	0.10	1335	2.97:1	0.65
mnf10a	10,000	100	1	0.16	335	0.74:1	0.30	680	1.51:1	0.30
mnf10b	10,000	100	1	0.04	515	1.14:1	0.10	935	2.08:1	0.40
mnf10c	10,000	100	1	0.08	385	0.86:1	0.10	745	1.66:1	0.35
mnf5a	5,000	100	1	0.16	355	0.79:1	0.10	550	1.22:1	0.30
mnf5b	5,000	100	1	0.04	460	1.02:1	0.10	645	1.43:1	0.30
mnf5 c	5,000	100	1	0.08	360	0.80:1	0.10	590	1.31:1	0.30
mnfv30a	30,000	100	1	0.16	390	0.87:1	0.15	1315	2.92:1	0.60
mnm30a	30,000	100	5	0.16	360	0.80:1	0.18	835	1.86:1	0.48
mnm30c	30,000	100	5	0.08	505	1.12:1	0.10	850	1.89:1	0.54
mnm10a	10,000	100	5	0.16	325	0.72:1	0.20	510	1.13:1	0.20
mnm10b	10,000	100	5	0.04	485	1.08:1	0.10	585	1.30:1	0.10
mnm10c	10,000	100	5	0.08	360	0.80:1	0.10	485	1.08:1	0.25
mnm5a	5,000	100	5	0.16	335	0.74:1	0.10	400	0.89:1	0.10
mnm5b	5,000	100	5	0.04	385	0.86:1	0.10	430	0.96:1	0.10
mnm5c	5,000	100	5	0.08	355	0.79:1	0.10	365	0.81:1	0.10
mnmv30a	30,000	100	5	0.16	365	0.81:1	0.27	1365	3.03:1	0.27
mns30a	30,000	100	10	0.16	360	0.80:1	0.17	960	2.13:1	0.32
mns20a	20,000	100	10	0.16	335	0.74:1	0.22	835	1.86:1	0.24
mns20c	20,000	100	10	0.08	435	0.97:1	0.10	835	1.86:1	0.15
mns10a	10,000	100	10	0.16	325	0.72:1	0.10	490	1.09:1	0.10
mns10b	10,000	100	10	0.04	460	1.02:1	0.10	505	1.12:1	0.10
mns10c	10,000	100	10	0.08	360	0.80:1	0.10	500	1.11:1	0.10
mnsv30a	30,000	100	10	0.16	355	0.79:1		710	1.58:1	

Table 4
Summary Statistics

Variable	L_e	L_c	C_e	C_c
Sample size	76	76	76	76
Average	564 feet	386 feet	0.27	0.11
Median	510 feet	360 feet	0.30	0.10
Standard deviation	249 feet	86 feet	0.15	0.06
Minimum	260 feet	275 feet	0.10	0.10
Maximum	1600 feet	655 feet	0.65	0.50
Range	1340 feet	380 feet	0.55	0.40

The regression relationships were required to express L_e, L_c, C_e, and C_c as functions of independent hydraulic variables which could be easily evaluated by the users of a one-dimensional model such as HEC-RAS. Some of the independent variables used in the regression analysis, such as discharge, slope, and roughness, had been set in defining each case. The other variables, such as Froude numbers, discharge distributions, velocities, depths, and conveyances, were evaluated from the HEC-RAS models which had been developed for each case. The raw independent variables were then entered into a spreadsheet. In the spreadsheet other variables were created as ratios and multiples of some of the raw variables.

After the spreadsheet of independent variables was complete, it was saved as an ASCII text file, which was in turn converted into a STATGRAPHICS data file. Only the cases with symmetric openings and spill-through abutments were included in the regression analyses. Those cases which had asymmetric openings or vertical abutments were later compared with the corresponding symmetric, spill-through cases.

The following sections present the regression equations resulting from the analysis of the data. In Equations 20 and 21 the dependent variable and all of the independent variables are non-dimensional. In Equations 17 through 19, however, the variables have mixed units of length and discharge. Consideration was given to casting all of the variables for these equations as non-dimensional, for instance by dividing all of the length variables by some reference length and the discharge by some reference discharge.

This idea was dismissed for several reasons. First, it would not in any way improve the regression results, and it may not be as straightforward for the practicing engineer to interpret. Second, there was no obvious discharge value by which to divide the discharge. Each model had only one discharge associated with it. Third, the only logical reference length would be the bridge opening width. Since this width is directly related to the average obstruction length, and both the dependent variable and one independent variable would be divided by this quantity, this action would cause a spurious correlation between the dependent variable and the average obstruction length variable.

In order for the information in this report to be useful to engineers working in the International System of Units (SI) Equations 17, 18, and 19, presented in the following sections, were also developed in SI units. The SI versions of these equations (Equations 17B, 18B, and 19B) are given in Appendix B.

7.2   Expansion Reach Lengths

In Table 3 it can be seen that the expansion ratio was less than 4:1 for all of the idealized cases. The mean and median values of the expansion ratio for the idealized cases were both around 1.5:1. The idealized cases included a wide range of hydraulic and geometric conditions. These observations are quite interesting because they indicate that the traditional 4:1 rule of thumb will over predict the expansion reach length for most situations.

Many independent variables and combinations of variables were investigated in seeking a possible correlation with L_e. The variable which showed the greatest correlation was the ratio of

the main channel Froude number at the most constricted section (Section 2) to that at the normal flow section (Section 1). The best-fitting equation for the expansion reach length is:

$$L_e = -298 + 257 \left(\frac{F_{c2}}{F_{c1}} \right) + 0.918 \left(\overline{L}_{obs} \right) + 0.00479 \left(Q \right) \qquad (17)$$

for which $\overline{R}^2 = 0.84$ and $S_e = 96$ feet, with

L_e = length of the expansion reach, in feet,

F_{c2} = main channel Froude number at Section 2,

F_{c1} = main channel Froude number at Section 1,

$\overline{L}_{obs}$ = average length of obstruction caused by the bridge approaches, in feet,

Q = total discharge, cfs,

$\overline{R}^2$ = the adjusted determination coefficient (the percentage of variance of the dependent variable from the mean which is explained by the regression equation), and

S_e = standard error of estimate.

Similarly, the regression equation for the expansion ratio was found to be

$$ER = \frac{L_e}{L_{obs}} = 0.421 + 0.485 \left(\frac{F_{c2}}{F_{c1}} \right) + 1.80 \times 10^{-5} \left(Q \right) \qquad (18)$$

for which $\overline{R}^2 = 0.71$ and $S_e = 0.26$.

Figure 10 and Figure 11 are plots of the observed values versus those predicted by the regression equations for L_e and ER, respectively. As indicated by the plots, Equation 17 fits the data better than Equation 18, although both fit reasonably well. An advantage of Equation 18 is that it has greater potential for general applicability over a broad range of scales, since it provides a ratio rather than an actual length. Both figures show one data point far to the right and far above all the other data points. This point is for case mnf30b, which had the highest discharge, the flattest slope, the narrowest bridge opening, and the smoothest overbanks of all of the regression cases. This is the case which would be expected to have the longest expansion reach, given the trends evident in Table 3. Because the data point representing case mnf30b is so far from the others in the plot, a regression analysis was performed with this point absent from the data. The resulting equation for expansion reach length, which was in the same variables as Equation 17, had an $\overline{R}^2$ value of 0.79 and an S_e value of 96 feet.

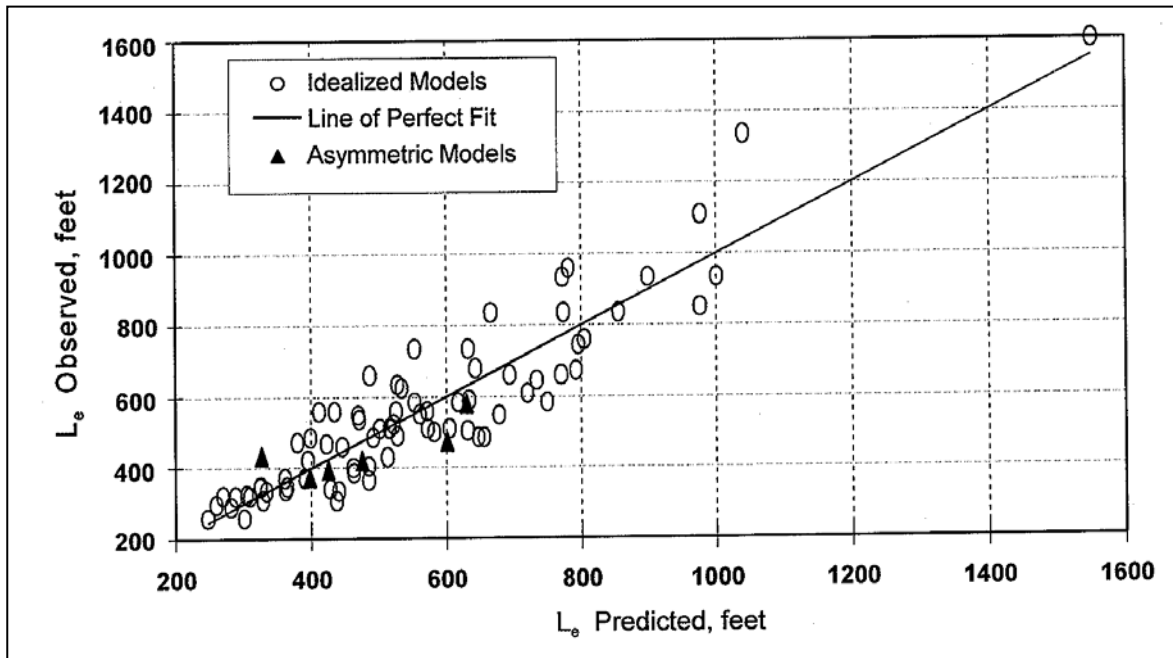**Figure 10** Goodness-of-Fit Plot for Expansion Length Regression Equation (Equation 17).
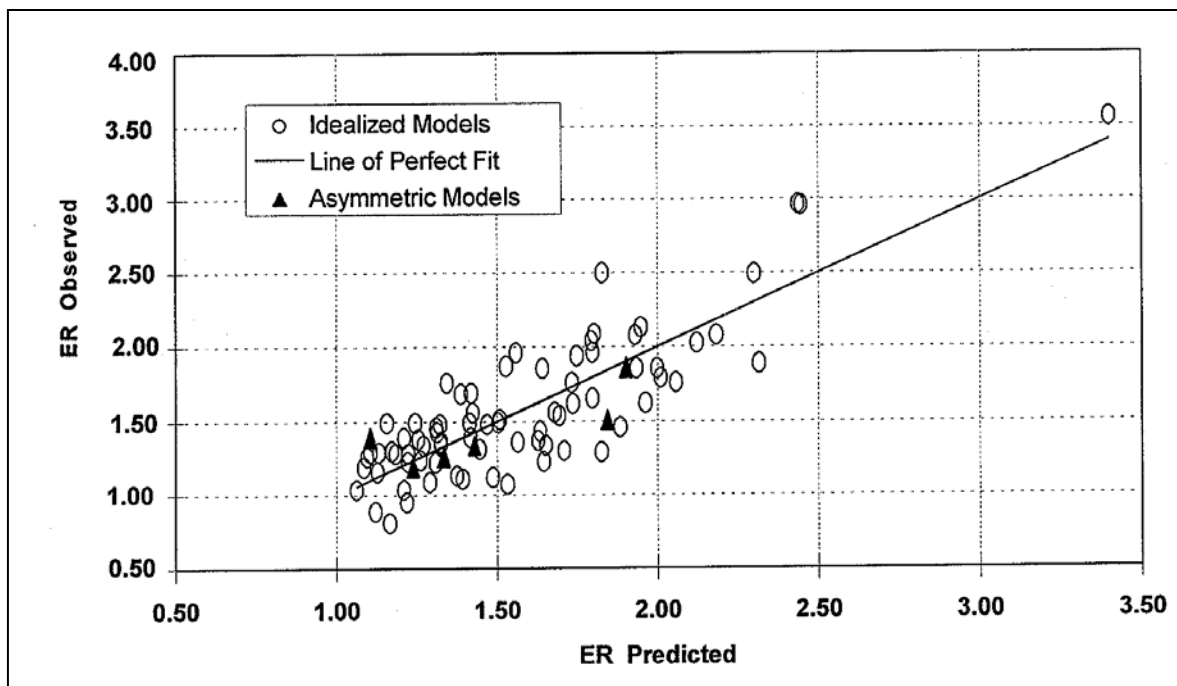

Figure 11 Goodness-of-Fit Plot for Expansion Ratio Regression Equation (Equation 18).

7.3   Contraction Reach Lengths

In contrast to the expansion reach length results, the results for contraction lend some support to the traditional rule of thumb which recommends the use of a 1:1 contraction ratio. The range

of values for this ratio was from 0.7:1 to 2.3:1. The median and mean values were both around 1.1:1.

The Froude number ratio in the previous two equations also proved to be significant in its relationship to the contraction reach length. Surprisingly, the Froude number ratio which involved the upstream (Section 4) Froude number did not have as strong a correlation as the one involving the Section 1 value. Here again the degree of constriction, in comparison with the undisturbed flow condition, is of high significance. The most significant independent variable for this parameter, however, was the percentage of the total discharge conveyed by the two overbanks. The best-fit equation from the regression analysis is

$$L_c = 263 \ + \ 38.8 \left(\frac{F_{c2}}{F_{c1}} \right) \ + \ 257 \left(\frac{Q_{ob}}{Q} \right)^2 \ - \ 58.7 \left(\frac{n_{ob}}{n_c} \right)^{0.5} \ + \ 0.161 \left(\overline{L}_{obs} \right) \qquad (19)$$

with $\overline{R}^2 = 0.87$ and $S_e = 31$ feet. In this equation

Q_{ob} = the discharge conveyed by the two overbank sections, in cfs, and

n_{ob} = the Manning n value for the overbank sections.

Figure 12 shows the observed versus predicted values for Equation 19.
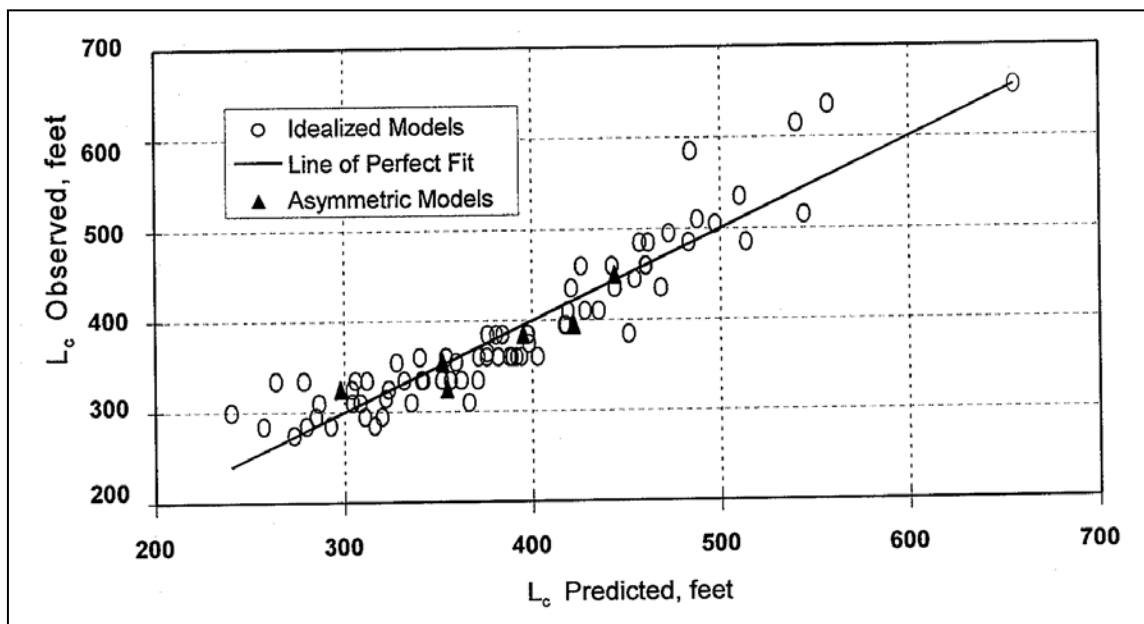
Figure 12 Goodness-of-Fit Plot for Contraction Reach Length Regression Equation (Equation 19).

The contraction length values did not vary much as a function of the bridge opening width or the average obstruction length. As a result most of the cases with the widest opening width, and therefore the shortest average obstruction length, had the highest contraction ratios. The numerator of the ratio varied only slightly while the denominator varied greatly. None of the

46

attempted regression relationships were good predictors of the contraction ratio. Equation 20 provided the best fit of all the combinations of independent variables tried. Figure 13 is a plot of the observed versus predicted values of the contraction ratio. The regression equation for the contraction ratio is:

$$CR = 1.4 \; - \; 0.333 \left(\frac{F_{c2}}{F_{c1}} \right) \; + \; 1.86 \left(\frac{Q_{ob}}{Q} \right)^2 \; - \; 0.19 \left(\frac{n_{ob}}{n_c} \right)^{0.5} \tag{20}$$
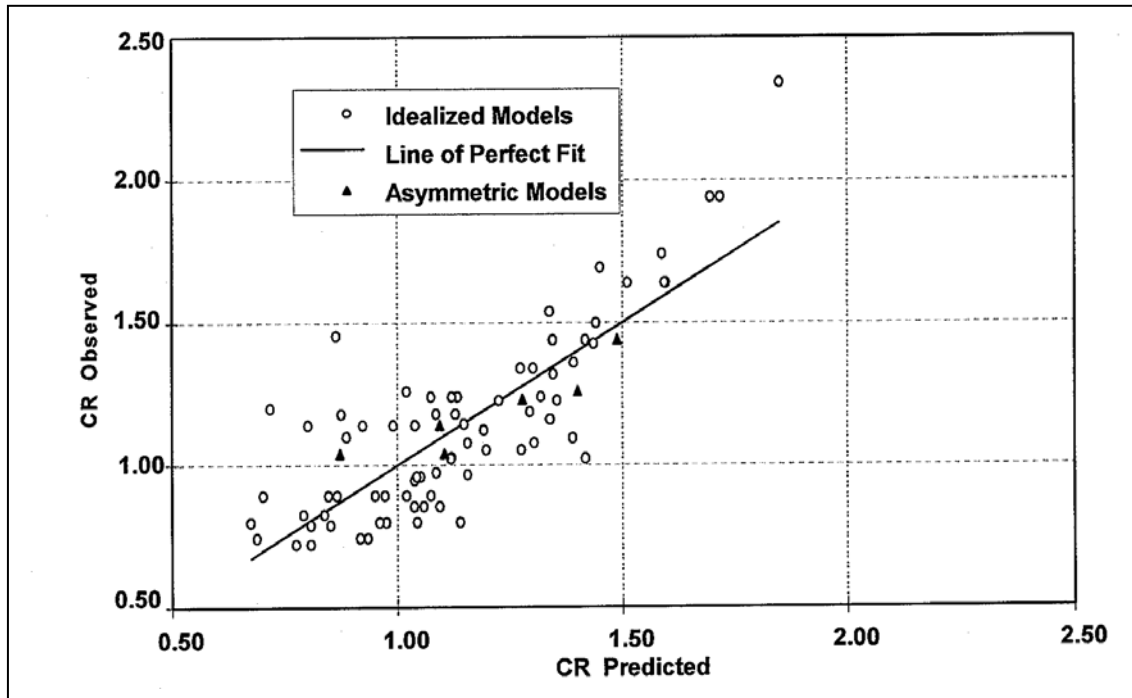
Figure 13 Goodness-of-Fit Plot for Contraction Ratio Regression Equation (Equation 20).

This equation has an $\overline{R}^2 = 0.65$ and $S_e = 0.19$. An unfortunate feature of this equation is the negative sign on the Froude number ratio term. This negative term indicates that the contraction ratio should become smaller as the constriction gets more severe. While this is in fact the case for the regression data, the general application of this equation to field sites should be done with caution.

7.4   Expansion Coefficients

Unlike the transition reach lengths, the transition coefficients did not lend themselves to strong regression relationships. This situation is partly due to the fact that the velocity head differences were as small in many instances as to render the coefficient values insignificant. Calibration of the coefficients under these conditions is obviously meaningless. Despite these difficulties, some trends were apparent in the expansion coefficient. The ratio of the hydraulic depth on the overbanks to the hydraulic depth in the main channel showed some correlation with C_e. The best regression relationship was

47

$$C_e = -0.092 + 0.570 \left(\frac{D_{ob}}{D_c} \right) + 0.075 \left(\frac{F_{c2}}{F_{c1}} \right) \qquad (21)$$

for which $\overline{R}^2 = 0.55$ and $S_e = 0.10$, with

D_{ob} = hydraulic depth (flow area divided by top width) for the overbank at the normal flow section (Section 1), in feet, and

D_c = hydraulic depth for the main channel at the normal flow section (Section 1), in feet.

Figure 14 shows the goodness of fit for this equation.
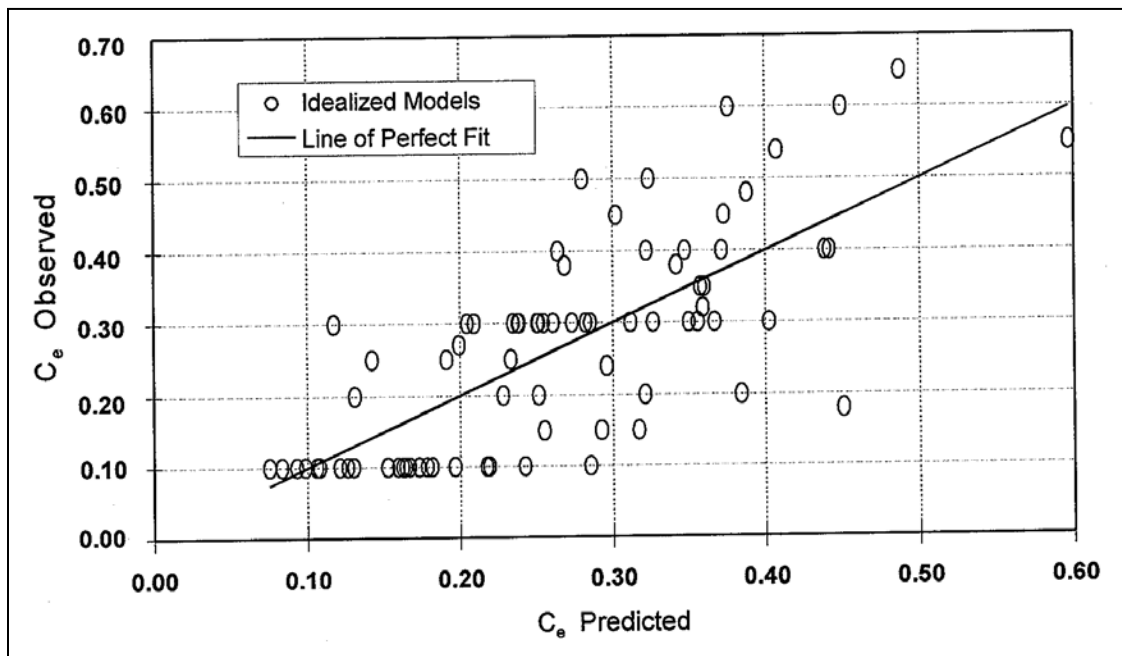
Figure 14   Goodness-of-Fit Plot for Expansion Coefficient Regression Equation (Equation 21).

The calibrated expansion coefficients ranged from 0.1 to 0.65. The median value was 0.3. Recalling that the traditional rule of thumb for this coefficient suggests a standard value of 0.5, it appears that the application of this rule could lead to an over prediction of energy loss in the expansion reach.

7.5   Contraction Coefficients

Of the 76 cases used in the regression analysis (those with symmetric openings and spill-through abutments), 69 had calibrated C_c values of 0.10. These included cases for which the contraction coefficient had no appreciable significance, as well as the 28 cases wherein the RMA-2 water surface elevation at the approach section was too low to be reached in HEC-RAS. Because of these conditions, the regression analysis was unfruitful. In addition to the regression

study with all of the data, an attempt at regression was made which incorporated only 20 cases. For this analysis those cases in which the contraction coefficient was inconsequential were omitted. This attempt also failed to yield a satisfactory regression relationship because 13 of these 20 cases still had calibrated coefficient values of 0.10.

The values for the contraction coefficient ranged from 0.10 to 0.50. The mean was 0.12 and the median value obviously was 0.10. Here again is a suggestion that the traditional standard value for bridges, in this case 0.30, is usually too high.

7.6   Asymmetric Cases

Six of the idealized cases modeled addressed the flow through asymmetric openings. Each case corresponded to a wide-opening case and a medium-opening case of the same discharge, slope, and roughness. The reason for running these models was to determine whether the averages of the L_e, L_c, C_e, and C_c values for the corresponding symmetric cases closely approximated the observed values for the asymmetric cases. Table 5 summarizes the results of the asymmetric case investigation. In Table 5, all case names contain the letter "a" which designates them as asymmetric cases. Also, the asymmetric cases are plotted with a special symbol on Figures 10 through 13. These results indicate that the relationships determined in this study for the symmetric cases apply equally well to asymmetric cases.

Table 5
Record of Data for Asymmetric Cases

Case	Q (cfs)	b (feet)	S (ft/mile)	n_{ob}	Contraction			Expansion		
					L_c (feet)	CR	C_c	L_e (feet)	ER	C_e
mam30c	30,000	375	5	0.08	395	1.26:1	0.10	473	1.51:1	0.50
mam10c	10,000	375	5	0.08	325	1.04:1	0.10	395	1.26:1	0.20
mam5c	5,000	375	5	0.08	325	1.04:1	0.10	435	1.39:1	0.10
maf30c	30,000	375	1	0.08	450	1.44:1	0.10	580	1.86:1	0.30
maf10c	10,000	375	1	0.08	385	1.23:1	0.10	420	1.34:1	0.30
maf5c	5,000	375	1	0.08	355	1.14:1	0.10	373	1.19:1	0.30

7.7   Vertical-Abutment Cases

Eleven idealized cases were studied with vertical abutments instead of spill-through abutments. Each of these cases corresponded to one spill-through case which had the same opening width, discharge, slope, and roughness. The models were created to determine what effect, if any, the difference in abutment shape had on the lengths of the transition reaches and the values of the transition coefficients. The results of the study of vertical-abutment cases are included in Table 3 (a) through (c). Except for the narrow-opening cases, the vertical abutments had no appreciable effect on the results, which indicates that the presence of vertical rather than

spill-through abutments should not discourage one from applying the relationships reported herein.

The narrow-opening vertical-abutment models had square corners at the upstream and downstream edges which resulted in very poor continuity performance in the RMA-2 models for these cases. Existing finite element two-dimensional hydrodynamic programs, including RMA-2, are not formulated to handle such difficult boundary conditions. The results from these simulations are therefore not considered to be accurate.

Chapter 8

Verification

Verification studies were conducted to test the validity and the applicability of the relationships reported in Chapter 7. The reliability of Equations 16 through 20 to produce parameter values leading to accurate one-dimensional water surface profiles within the range of the independent variables in the regression analyses was tested. Also, the applicability of the equations to field sites was investigated. Two-dimensional models of additional idealized cases, with larger and smaller floodplain widths, were also created and used to test the applicability of Equations 16 through 20 to floodplains of different sizes. Finally, the effects of the finite element mesh density and the eddy viscosity values on the RMA-2 results were studied.

8.1   Reliability Within the Range of Regression Data

Four of the HEC-RAS models for the idealized cases (all of which had previously been calibrated for best agreement with the corresponding RMA-2 models) were modified to reflect the cross section locations and expansion coefficient determined by the regression relationships. The resulting water surface elevations at Sections 4 and 2 were compared with the values for each corresponding RMA-2 model and calibrated HEC-RAS model.

The four cases that were used in this activity included three symmetric cases, mmf30b, mms10b, mnf30c, and one asymmetric case, mam10c. The first three of these cases all have an error of estimate for the expansion reach length above 100 feet. One of the cases has an error of estimate for the contraction reach length of nearly 80 feet. The inclusion of some cases with high errors of estimate for the reach lengths was done intentionally in order to determine the magnitude of the detrimental effect that these errors have on the water surface profiles.

In all four of the cases tested, the water surface elevations at Sections 4 and 2, resulting from the use of the Equations 17, 19, and 21, were within 0.2 feet of those in the calibrated HEC-RAS models. Equations 18 and 20, for the expansion ratio and contraction ratio, were not incorporated into the modified HEC-RAS models. These results lead to the conclusion that the use of Equations 17, 19, and 21 will reliably lead to water surface profiles of adequate accuracy within the range of the conditions found in the cases which were used to develop the regression equations. This assumes, of course, that the model is accurate in all other respects, such as the estimates of roughness and discharge.

8.2   Applicability to Field Sites

The calibrated HEC-RAS models from four of the field sites mentioned in Section 3.3 of Chapter 3 were used to test the applicability of the regression equations to field data. As in the application to the idealized cases, Equations 17, 19, and 21 were of primary interest. The sites and events that were used in this exercise are summarized in Table 6.

Table 6
Field Sites Used for Verification

Site	Discharge (cfs)	Floodplain Width (feet)
Alexander Creek, Alabama	9500	950
Bogue Chitto, Mississippi	31500	4500
Buckhorn Creek, Alabama	4150	1400
Tenmile Creek, Louisiana	6400	2000

The expansion and contraction ratios in the calibrated models of the four field sites were all less than 1:1. The expansion ratios that were computed using the reach lengths predicted by Equation 17 ranged from 1:1 to 1.5:1. The RMA-2 model of Buckhorn Creek (see Section 5.1 of Chapter 5) indicated an expansion ratio of 1.3:1. The computed expansion ratio for Buckhorn Creek was 1.3:1, according to Equation 16.

Using the reach lengths predicted by Equation 19, the computed contraction ratios ranged from 0.2:1 to 1.5:1. The site for which the computed contraction ratio was 0.2 is Bogue Chitto, which has a floodplain width of approximately 4500 feet. The contraction ratio from the RMA-2 model of Buckhorn Creek was 0.7:1 while that computed by Equation 19 was 1.5:1. Equation 20 was also tested on each of these sites. It predicted contraction ratios much larger than those resulting from Equation 19.

While there were some differences in the contraction and expansion reach lengths, the HEC-RAS water surface profiles resulting from the use of Equations 17, 19, and 21 were reasonably close to the calibrated models. The largest disparity in the Section 4 water surface elevation was 0.8 feet in the Bogue Chitto model which was much wider than the others. In the other three models, the computed Section 4 water surface elevations using the regression equations were all within 0.5 feet of the calibrated models. When the overall width of the prototype floodplain is near 1000 feet, say 800 to 1500 feet, and the other parameters, such as discharge, roughness, and slope are within the range used in this study, one can conclude that Equations 17, 18, 19, and 21 can be applied to field sites with confidence. On the other hand, Equation 20 performed poorly for these sites, consistently over predicting the contraction ratio to a significant degree.

8.3   Applicability to Larger Scales

Two-dimensional models were created for two idealized cases with a 5000-foot floodplain width. Each of the large cases corresponded to a 1000-foot wide case with the same slope and Manning n values. The discharges in the large cases were those which flowed at normal depths equal to five times the normal depths of the corresponding 1000-foot wide cases. In both of these large cases the discharge of the 1000-foot case was 30,000 cfs and the corresponding discharge in the scaled models was 2,193,000 cfs. It was found that the scale factor for discharge that was required to produce proportional normal depths was equal to the spatial scale factor raised to the power of 2.67.

These two large cases both had bridge opening widths of 1,250 feet, which corresponded to the medium opening width cases. One case, 1mm22a, had a slope of 5 feet/mile with an overbank Manning n value of 0.16, corresponding to case mmm30a. The other, 1mf22c, had a slope of 1 foot/mile with an overbank n value of 0.08, corresponding to case mmf30c. The eddy viscosity multipliers were set as low as possible without producing an unstable computation.

After the RMA-2 models for both cases had been computed, the expansion and contraction reach lengths were determined by the methods described in Chapter 5. For each case the HEC-RAS model was calibrated for the best match with the RMA-2 water surface elevations. The calibrated HEC-RAS models reflected the reach lengths taken from the RMA-2 results, and the expansion and contraction coefficients were the calibration parameters. As with many of the 1000-foot cases studied, the HEC-RAS water surface elevations upstream from the bridge were higher than the corresponding RMA-2 water surface elevations. With C_c set at zero for both cases, the approach section water surface elevation difference was 5.9 feet (5% of the depth) for lmm22a and 2.7 feet (2% of the depth) for 1mf22c.

For case lmm22a the expansion length was 2,700 feet, which corresponds to an expansion ratio of 1.4:1, and the contraction length was 2,000 feet, for a contraction ratio of 1.1:1. In case lmf22c the expansion distance was 4,700 feet and the contraction distance was 2,900 feet, giving expansion and contraction ratios of 2.5:1 and 1.5:1, respectively.

Equation 16 predicted expansion distances of 12,400 feet and 12,600 feet respectively for the 5 feet/mile and 1 foot/mile cases respectively, overestimating the distance by more than a factor of two in both cases. The discharge-related term in Equation 17 had a value of 10,500 for both cases, obviously dominating the predicted values. Equation 18 performed less well, giving expansion ratios greater than 40:1 for both cases. Here again the discharge term of the equation dominated the prediction, with a value of 39.5 for both cases. Table 7 summarizes the expansion distance observations and predictions for the large cases.

Table 7
Large Cases: Expansion Distances and Ratios

Case	L_e (RMA-2)	ER (RMA-2)	L_e (Eqn. 17)	ER (Eqn. 18)
1mm22a	2700	1.4:1	12400	40.9:1
1mf22c	4700	2.5:1	12600	41.7:1

These results show that Equations 17 and 18 will over predict the expansion distance in cases where the discharge is significantly greater than 30,000 cfs. The discharge value of 2,193,000 cfs, while producing the desired scaled dimensions for comparison with the corresponding cases in the regression group, is unrealistic considering that the peak discharge observed in the Mississippi River flooding of 1993 was less than 1,500,000 cfs. Even if a value of 1,000,000 cfs were used, however, the discharge terms in Equations 17 and 18 would still produce a significant over prediction.

This over prediction led to the development of another equation for the expansion ratio for possible application to large-scale cases. The equation was developed via a regression analysis of the full data set of symmetric, spill-through 1000-foot wide cases and is given below:

$$ ER = \frac{L_e}{L_{obs}} = 0.489 \ + \ 0.608 \left(\frac{F_{c2}}{F_{c1}} \right) \tag{22} $$

The adjusted determination coefficient and standard error of estimate are $\overline{R}^2 = 0.59$ and $S_e = 0.31$. This equation predicted an expansion ratio of 1.7:1 for 1mm22a, which is too large, and 2.1:1 for 1mf22c, which is too small.

Equation 19, for predicting the contraction distances, has no discharge-related term. It predicted contraction distances of 620 and 690 feet for 1mm22a and 1mf22c, respectively. Both predicted values were less than a third of the recorded values. This length-based equation has no mechanism, except for the average obstruction length term, to respond to significant scale changes.

The equation for contraction ratio prediction, Equation 20, was applied to these cases and predicted ratios of 1.05:1 and 1.29:1 for 1mm22a and 1mf22c, respectively. These predictions compare rather well with the observed values. As discussed in Section 7.3 of Chapter 7, however, Equation 20 is suspect due to the sign of the Froude number ratio term. Another possibility that was investigated was multiplying the Equation 19 predictions by the length-scale factor. This resulted in predicted lengths of 3,080 feet for 1mm22a and 3,445 feet for 1mf22c. Table 8 summarizes the contraction distance observations and predictions for the large cases.

Table 8
Large Cases: Contraction Distances and Ratios

Case	L_c (RMA-2)	CR (RMA-2)	L_c (Eqn. 19)	CR (Eqn. 20)
1mm22a	2000	1.1:1	620	1.1:1
1mf22c	2950	1.6:1	690	1.3:1

The contraction lengths from the study of the large models show that Equation 18 will under predict the contraction length when it is applied to floodplains having a significantly larger width than 1,000 feet. Given the way the contraction length is defined (see Section 5.2.2 of Chapter 5), it may be rational to multiply the predictions of Equation 19 by the scale factor, but more data from larger cases would be required to determine this conclusively.

The values of C_e determined from calibrating the HEC-RAS models were 0.55 for 1mm22a and 0.50 for 1mf22c. The values predicted by Equation 21, which predicts the expansion coefficient, were 0.40 and 0.46 respectively. These were both cases in which the value of the expansion coefficient was quite significant in the one-dimensional computations of the water surface elevation at the downstream face of the bridge.

The study of these large models indicated that Equations 17 and 18 should not be used to predict the expansion distance in cases where the discharge is much larger than 30,000 cfs. Also, Equation 19 should not be used to predict the contraction distances in cases where the floodplain width is much larger than 1,000 feet. It appears that the best approach at this time is to use Equation 21 for predicting the expansion distance and Equation 20 (with care) for predicting the contraction ratio. An HEC-RAS model was created for the 1mm22a case in which these recommendations were incorporated. The results of this model were only slightly worse than the calibrated model. The approach-section water surface elevation was 0.5 feet higher than that of the calibrated model, which was already 5.9 feet above the corresponding RMA-2 water surface.

The results of the large case RMA-2 models were compared directly with the corresponding 1000-foot wide cases. The comparison is shown in Table 9. The comparison shows a slight increase in both the expansion and contraction ratios corresponding to the increase in scale.

Table 9
Comparison of Large-Scale Cases to the
Corresponding 100-foot Cases

Case	Expansion Ratio	Contraction Ratio
mmm30a	1.3:1	1.0:1
1mm22a	1.4:1	1.1:1
mmf30c	2.0:1	1.3:1
1mf22c	2.5:1	1.6:1

8.4   Applicability to Smaller Scales

Models were also created for two idealized cases with a smaller overall width. In these cases the dimensions were scaled by a factor of 0.3 to create a floodplain width of 300 feet. The discharges in the small cases were those which flowed at normal depths equal to 0.3 times the normal depths of the corresponding 1000-foot wide cases. In one of the cases, smm12c, the discharge of the corresponding 1000-foot case was 30,000 cfs, and the discharge in the scaled case was 1200 cfs. In the other case, sms8c, the discharge was 810 cfs, corresponding to a discharge of 20,000 cfs in the 1000-foot case.

The two small cases that were modeled both had bridge opening widths of 75 feet, which corresponded to the medium opening width cases. Both of the smaller cases had an overbank Manning n value of 0.08. Case smm12c had a slope of 5 feet/mile, corresponding to case mmm30c, and case sms8c had a slope of 10 feet/mile, corresponding to case mms20c. Once again, the eddy viscosity multipliers were set as low as possible without creating an unstable computation.

For case smml2c the expansion reach length was 180 feet, which gives an expansion ratio of 1.6:1, and the contraction reach length was 115 feet, for a contraction ratio of 1.0:1. In case sms8c the expansion distance was 160 feet and the contraction distance was 110 feet, giving

expansion and contraction ratios of 1.4:1 and 1.0:1, respectively. Table 10 summarizes the observed and predicted expansion distances and ratios. Table 11 is a summary of the contraction values.

Table 10
Small Cases: Expansion Distances and Ratios

Case	L_e (RMA-2)	ER (RMA-2)	L_e (Eqn. 17)	ER (Eqn. 18)
smm12c	180	1.6:1	335	1.4:1
sms8c	160	1.4:1	290	1.4:1

Table 11
Small Cases: Contraction Distances and Ratios

Case	L_c (RMA-2)	CR (RMA-2)	L_c (Eqn. 19)	CR (Eqn. 20)
smm12c	115	1.0:1	400	1.4:1
sms8c	110	1.0:1	370	1.3:1

The ratio-based equations, Equation 18 for expansion and Equation 20 for contraction, were more accurate than the length-based equations in determining the transition reach lengths for these small-scale cases. Equations 17 and 19 both over predicted the reach lengths to a significant extent.

For both cases the HEC-RAS models were calibrated to the best match with the RMA-2 water surface elevations. The water surface elevations in the calibrated models were within 0.2 feet of the RMA-2 water surface at all sections. Once the models were calibrated, they were altered by incorporating the expansion ratio and contraction ratio predicted by Equations 18 and 20, respectively. At all sections in both cases, the detrimental effect on the water surface profile accuracy was less than or equal to 0.1 feet.

This study of smaller-scale cases leads to the conclusion that Equation 18 is an adequate predictor of the expansion ratio for cases in which the floodplain width and discharge are significantly less than the values used in the regression analysis. Equation 17, however, could be expected to over predict the length significantly. Equation 19 will also over predict the contraction reach length, unless modified by the scale factor. Equation 20 predicted reasonably accurate contraction ratios for these cases.

The results of the small-case RMA-2 models were compared directly with the corresponding 1000-foot wide cases. The comparison is shown in Table 12. The comparison shows a slight decrease in both the expansion and contraction ratios, corresponding to the decrease in scale.

Table 12
Comparison of Small-Scale Cases to the
Corresponding 1000-foot Cases

Case	Expansion Ratio	Contraction Ratio
mmm30c	1.8:1	1.2:1
smm12c	1.6:1	1.0:1
mms20c	1.6:1	1.1:1
sms8c	1.4:1	1.0:1

8.5   Effects of RMA-2 Model Refinement and Eddy Viscosity Coefficients

As discussed in Section 4.3 of Chapter 4, an important factor in the accurate modeling of flow fields with RMA-2 is the level of refinement of the finite element network. To investigate the sensitivity of the RMA-2 results of interest (the transition reach lengths and the water surface elevations) to network refinement, the network of one idealized case, mmm30a, was refined drastically in the immediate vicinity of the constriction.

The disparity between the HEC-RAS and RMA-2 water surface elevations upstream of the bridge in some of the studied cases was mentioned in Section 6.3 of Chapter 6. It was suspected that this disparity could be due in part to the fact that flow continuity is not perfectly preserved in the constricted region. Case mmm30a was chosen for the model refinement study because it is one of the cases where this problem was encountered.

The refinement of the network was accomplished by splitting the quadrilateral elements in the constricted area. They were first split in the longitudinal direction, halving the Δx dimension of each element; then they were split in the transverse direction, halving each element's Δy dimension. Then the necessary changes were made in the surrounding region of the mesh to preserve the connectivity of the elements and to avoid wherever feasible the adjacent placement of elements that differed in size by more than a factor of 2. The resulting finite element network had approximately 1900 elements, compared with the original element count of 1150. Perhaps more importantly, the maximum front width of the network was approximately doubled. The computational time of RMA-2 is proportional to the square of the front width.

After the model was run, the contraction and expansion reach limits were defined from the RMA-2 output in the manner described in Section 5.2 of Chapter 5. They were found to be equal to those recorded for the standard model of mmm30a. Furthermore, a version of the model which had eddy viscosity multiplier values more than 10 times higher than the ultimate values (the higher values were used initially to ease the model to the desired boundary conditions) showed no difference in transition reach lengths in comparison with the ultimate model.

The mass conservation performance of the model was slightly improved by refining the network. This effect is best described in Table 13, which expresses the continuity performance at various locations in the constricted area as percentages of the original upstream discharge.

57

The eddy viscosity coefficient multipliers in the ultimate refined model were equal to those in the standard model for case mmm30a. The eddy viscosity coefficients were found to have a less important effect on the continuity preservation of RMA-2. The model which used eddy viscosity coefficients which were ten times larger had slightly better continuity at some locations (approximately one percent) and no improvement at other locations.

Table 13
Effects of Network Refinement on RMA-2 Mass Conservation

Location	Continuity in mmm30a (%)	Continuity in Refined
just upstream of	97.3	97.8
upstream bridge face	92.8	95.2
centerline of bridge	93.6	96.4
downstream bridge	94.9	96.8
just downstream	103.0	98.2

Probably as a result of the improved continuity performance, the water surface elevation that was computed by RMA-2 at the approach section was 0.18 feet higher in the final refined model than in the standard model for the case. The gap between the RMA-2 and HEC-RAS approach section water surfaces was narrowed from 0.5 feet in the standard model to about 0.3 feet in the refined model.

This study showed that the transition reach lengths from the RMA-2 models were not sensitive to a doubling of the network density in the constricted area, nor were they sensitive to large changes in the eddy viscosity coefficients. The continuity performance of RMA-2 was improved by network refinement and to a lesser extent by higher eddy viscosity coefficients. The water surface elevations upstream of the bridge increased slightly for the refined model.

The refined model required four times as much computation time as the standard model. Considering the minor changes in the results versus the major increase in computation time, it clearly would not have been efficient to use a higher level of refinement for the standard models. Since the major refinement in this model closed the gap between the RMA-2 and HEC-RAS water surface results by only 0.2 feet out of 0.5, it appears likely that this gap cannot be completely closed by refinement of the network. This leads to the conclusion for the cases in which the disparity exists that the contraction coefficients should remain at the minimum value of 0.10. The disparity should be attributed to either a low bias in RMA-2 or a high bias in HEC-RAS, or both, in computing the energy loss in both the constricted reach and the contraction reach (between Sections 4 and 2).

Chapter 9

Conclusions and Recommendations

The goals of the research described in this report were to gain insight into the transition reaches at bridge constrictions and to develop improved guidance on the application of one-dimensional hydraulic models at bridges. Specifically, four modeling parameters were studied thoroughly. The lengths of the expansion and contraction reaches, L_e and L_c respectively, were investigated, along with the transition coefficients C_e and C_c.

9.1   Conclusions

The research has successfully provided valuable insight with regard to all four parameters of concern. Also, strong relationships between the expansion reach length, the contraction reach length and the expansion coefficient and the independent variables that affect them have emerged from the analysis of the idealized two-dimensional models. The insights gained and relationships determined from this study provide a basis for improved guidance in the bridge-related application of one-dimensional models such as HEC-RAS and HEC-2.

9.1.1   Expansion Reach Lengths

Of all of the two-dimensional cases created for this study, which included a wide range of hydraulic and geometric conditions, none of the cases had an expansion ratio as great as 4:1. Most of the cases had expansion ratios between 1:1 and 2:1. This indicates that a dogmatic use of the traditional 4:1 rule of thumb for the expansion ratio leads to a consistent over prediction of the energy losses in the expansion reach in most cases. The accompanying over prediction of the water surface elevation at the downstream face of the bridge may be conservative for flood stage prediction studies. For bridge scour studies, however, this overestimation of the tailwater elevation could in some circumstances lead to an underestimation of the scour potential.

The results from the two-dimensional models did not always indicate the presence of large-scale flow separations or eddy zones downstream of the bridge. Their presence corresponded with the larger values of L_e. For many of the cases there was no significant separation evident in the results. In sensitivity tests, the presence or absence of eddy zones was not sensitive to the eddy viscosity coefficient value. Likewise, eddy viscosity settings did not have an appreciable effect on L_e.

It was found that the ratios of the channel Froude number at Section 2 to that at Section 1 (F_{c2}/F_{c1}) correlated strongly with the length of the expansion reach. Regression equations were developed and given in Section 7.2 of Chapter 7 for both the expansion reach length and the expansion ratio. The equations are repeated later in this chapter. Both equations are linear and contain terms involving the Froude number ratio and the discharge. The equation for expansion

length also includes the average obstruction length in one term. To use these regression equations in the application of a one-dimensional model will usually require an iterative process since the hydraulic properties at Section 2 will not be known in advance. The effort involved in this process will not be large, however, because the method will usually converge rapidly.

The value of the Froude number ratio reflects important information about the relationship between the constricted flow and the normal flow conditions. It is in effect a measure of the degree of flow constriction since it compares the intensity of flow at the two locations. Since these Froude numbers are for the main channel only, the value of F_{c1} also happens to reflect to some extent the distribution of flow between the overbanks and main channel.

There was no support from these investigations for the WSPRO concept of the expansion reach length being proportional to or equal to the bridge opening width.

9.1.2   Contraction Reach Lengths

While the apparent contraction ratios of the five field prototype cases were all below 1:1, the contraction ratios for the idealized cases ranged from 0.7:1 to 2.3:1. As with the expansion reach lengths, these values correlated strongly with the same Froude number ratio. A more important independent variable, however, is the decimal fraction of the total discharge conveyed in the overbanks (Q_{ob}/Q) at the approach section. A strong regression equation was developed for the contraction length and is presented in Section 7.3 of Chapter 7 and repeated later in this chapter.

Because the mean and median values of the contraction ratios were both around 1:1, there is some support from this study for the rule of thumb which suggests the use of a 1:1 contraction ratio. There is no support, however, for the concept of the contraction reach length being equal to or proportional to the bridge opening width.

9.1.3   Expansion Coefficients

Regression analysis for this parameter was only marginally successful. The resulting relationship is a function of the ratio of hydraulic depth in the overbank to that in the main channel for undisturbed conditions (evaluated at Section 1). Perhaps more interesting are the summary statistics, which indicate lower values for this coefficient than the traditional standard values for bridges.

9.1.4   Contraction Coefficients

Owing to the nature of this data (69 out of 76 cases had the minimum value of 0.10), a regression analysis was not fruitful. Like the expansion coefficients, the prevailing values are significantly lower than the standard recommended values. To a small extent, the results for this parameter are suspect due to the disparity between the RMA-2 results and the HEC-RAS results for 28 of the cases. The study of a more refined RMA-2 model of one of the standard cases, which is described in Section 8.5 of Chapter 8, indicated that the disparity between the two

programs was only partially removed by drastically refining the network mesh (approximately 0.2 feet out of a 0.5 feet gap). The conclusion arising from the study of the effects of mesh refinement was that no practical amount of refinement would be sufficient to resolve completely the difference between the HEC-RAS and RMA-2 water surface elevations for most of these 28 cases. In other words, the calibrated value of the contraction coefficient would be at the minimum value of 0.10 even if the RMA-2 models were far more refined than those used in the standard cases.

9.1.5   Asymmetric Bridge Openings

For these data the averages of the reach length values for the two corresponding symmetric cases closely approximated the values determined for the asymmetric cases. When the regression equations for L_e, ER, and L_c were applied to the asymmetric cases, the predicted values were near the observed values, as illustrated by Figures 10, 11, and 12. This indicates that the regression relationships for the transition reach lengths can also be applied to asymmetric cases (that is, most real-world cases).

9.1.6   Vertical-Abutment Cases

For these data there was no major effect on the transition lengths or the coefficients due to the use of vertical rather than spill-through abutments. The exceptions to this statement were three vertical-abutment cases in the narrow-opening class for which square corners were used. The square-cornered abutments were a deliberate attempt to model a very severe situation. Because the RMA-2 program, or any two-dimensional numerical model for that matter, is not well-formulated to handle such drastic boundary conditions, no general conclusions should be drawn from these cases about actual field sites having such a configuration.

9.2   Recommendations

The remainder of this chapter presents recommendations arising from the results documented in Chapter 7 and the verification efforts discussed in Chapter 8. These recommendations are intended to provide the users of one-dimensional water surface profile programs, such as HEC-RAS, with guidance in the application of the programs to the modeling of transitions in bridge hydraulics problems. These recommendations supplement the user documentation for HEC-RAS (HEC, 1995b and 1995c) which provides detailed guidance on the modeling of flows at bridges.

In applying these recommendations, the modeler should always consider the range of hydraulic and geometric conditions included in the data. Wherever possible, the transition reach lengths used in the model should be validated by field observations of the site in question, preferably under conditions of high discharge. The evaluation of contraction and expansion coefficients should ideally be substantiated by site-specific calibration data, such as stage-discharge measurements just upstream of the bridge. The following recommendations are given

in recognition of the fact that site-specific field information is often unavailable or very expensive to obtain.

9.2.1   Expansion Reach Lengths

In some types of studies, a high level of sophistication in the evaluation of the transition reach lengths is not justified. For such studies, and for a starting point in more detailed studies, Table 14 offers ranges of expansion ratios which can be used for different degrees of constriction, different slopes, and different ratios of overbank roughness to main channel roughness. Once an expansion ratio is selected, the distance to the downstream end of the expansion reach (the location of Section 1 on Figure 1) is found by multiplying the expansion ratio by the average obstruction length. The average obstruction length is half of the total reduction in floodplain width caused by the two bridge approach embankments. In Table 14, b/B is the ratio of the bridge opening width to the total floodplain width, n_{ob} is the Manning n value for the overbank, n_c is the n value for the main channel, and S is the longitudinal slope. The values in the interior of the table are the ranges of the expansion ratio. For each range, the higher value is typically associated with a higher discharge.

Table 14
Ranges of Expansion Ratios

		$\dfrac{n_{ob}}{n_c} = 1$	$\dfrac{n_{ob}}{n_c} = 2$	$\dfrac{n_{ob}}{n_c} = 4$
b/B=0.10	S=1	1.4 - 3.6	1.3 - 3.0	1.2 - 2.1
	5 ft/mile	1.0 - 2.5	0.8 - 2.0	0.8 - 2.0
	10 ft/mile	1.0 - 2.2	0.8 - 2.0	0.8 - 2.0
b/B=0.25	1 ft/mile	1.6 - 3.0	1.4 - 2.5	1.2 - 2.0
	5 ft/mile	1.5 - 2.5	1.3 - 2.0	1.3 - 2.0
	10 ft/mile	1.5 - 2.0	1.3 - 2.0	1.3 - 2.0
bB = 0.50	1 ft/mile	1.4 - 2.6	1.3 - 1.9	1.2 - 1.4
	5 ft/mile	1.3 - 2.1	1.2 - 1.6	1.0 - 1.4
	10 ft/mile	1.3 - 2.0	1.2 - 1.5	1.0 - 1.4

The ranges in Table 14, as well as the ranges of other parameters to be presented later in this chapter, capture the ranges of the idealized model data from this study. Another way of establishing reasonable ranges would be to compute statistical confidence limits (such as 95% confidence limits) for the regression equations. Confidence limits in multiple linear regression equations have a different value for every combination of values of the independent variables (Haan, 1977). The computation of these limits entails much more work and has a more restricted range of applicability than the corresponding limits for a regression which is based on only one independent variable. The confidence limits were, therefore, not computed in this study.

Extrapolation of expansion ratios for constriction ratios, slopes or roughness ratios outside of the ranges used in this table should be done with care. The expansion ratio should not exceed 4:1, nor should it be less than 0.5:1 unless there is site-specific field information to substantiate

such values. The ratio of overbank roughness to main-channel roughness provides information about the relative conveyances of the overbank and main channel. The user should note that in the data used to develop these recommendations, all cases had a main-channel n value of 0.04. For significantly higher or lower main-channel n values, the n value ratios will have a different meaning with respect to overbank roughness. It is impossible to determine from the data of this study whether this would introduce significant error in the use of these recommendations.

When modeling situations which are similar to those used in the regression analysis, with floodplain widths near 1,000 feet, bridge openings between 100 and 500 feet wide, and slopes between one and ten feet per mile, the regression equation for the expansion reach length can be used with confidence. Equation 17 is repeated here for convenience.

$$L_e = -298 \; + \; 257 \left(\frac{F_{c2}}{F_{c1}} \right) \; + \; 0.918 \left(\overline{L}_{obs} \right) \; + \; 0.00479 \left(Q \right) \tag{17}$$

where

L_e =   length of the expansion reach, in feet,

F_{c2} =   main channel Froude number at Section 2,

F_{c1} =   main channel Froude number at Section 1,

$\overline{L}_{obs}$ =   average length of obstruction caused by the bridge approaches, in feet,

Q =   total discharge, cfs,

When the width of the floodplain and the discharge are smaller than those of the regression data, the expansion ratio can be estimated by Equation 18. The computed value should be checked against ranges in Table 14. Equation 18 is

$$ER = \frac{L_e}{L_{obs}} = 0.421 \; + \; 0.485 \left(\frac{F_{c2}}{F_{c1}} \right) + \; 1.80 \times 10^{-5} \left(Q \right) \tag{18}$$

When the scale of the floodplain is significantly larger than that of the data, particularly when the discharge is much higher than 30,000 cfs, Equations 17 and 18 will overestimate the expansion reach length. Equation 22 should be used in such cases, but again the resulting value should be checked against the ranges given in Table 14:

$$ER = \frac{L_e}{L_{obs}} = 0.489 \; + \; 0.608 \left(\frac{F_{c2}}{F_{c1}} \right) \tag{22}$$

The depth at Section 2 is dependent upon the expansion reach length, and the Froude number at the same section is a function of the depth. This means that an iterative process is required to use the three equations above, as well as the equations presented later in this chapter for

63

contraction reach lengths and expansion coefficients. It is recommended that the user start with an expansion ratio from Table 14, locate Section 1 according to that expansion ratio, set the main channel and overbank reach lengths as appropriate, and limit the effective flow area at Section 2 to the approximate bridge opening width. The program should then be run and the main channel Froude numbers at Sections 2 and 1 read from the model output. Use these Froude number values to determine a new expansion length from the appropriate equation, move Section 1 as appropriate and recompute. Unless the geometry is changing rapidly in the vicinity of Section 1, no more than two iterations after the initial run should be required.

When the expansion ratio is large, say greater than 3:1, the resulting reach length may be so long as to require intermediate cross sections which reflect the changing width of the effective flow area. These intermediate sections are necessary to reduce the reach lengths when they would otherwise be too long for the linear approximation of energy loss that is incorporated in the standard step method. These interpolated sections are easy to create in the HEC-RAS program, because it has a graphical cross section interpolation feature. The importance of interpolated sections in a given reach can be tested by first inserting one interpolated section and seeing the effect on the results. If the effect is significant, the subreaches should be subdivided into smaller units until the effect of further subdivision is inconsequential.

9.2.2 Contraction Reach Lengths

Ranges of contraction reach lengths for different conditions are presented in Table 15 for use as starting values and for studies which do not justify a sophisticated evaluation of the contraction reach length. Note that this table does not differentiate the ranges on the basis of the degree of constriction. For each range the higher values are typically associated with higher discharges and the lower values with lower discharges.

Table 15
Ranges of Contraction Ratios

		$\dfrac{n_{ob}}{n_c} = 1$	$\dfrac{n_{ob}}{n_c} = 2$	$\dfrac{n_{ob}}{n_c} = 4$
S	= 1 ft/mile	1.0 - 2.3	0.8 - 1.7	0.7 - 1.3
	5 ft/mile	1.0 - 1.9	0.8 - 1.5	0.7 - 1.2
	10 ft/mile	1.0 - 1.9	0.8 - 1.4	0.7 - 1.2

When the conditions are within or near those of the data, the contraction reach length regression equation (Equation 19, repeated here for convenience) may be used with confidence:

$$L_c = 263 + 38.8 \left(\frac{F_{c2}}{F_{c1}} \right) + 257 \left(\frac{Q_{ob}}{Q} \right)^2 - 58.7 \left(\frac{n_{ob}}{n_c} \right)^{0.5} + 0.161 \left(\bar{L}_{obs} \right) \qquad (19)$$

64

In this equation

$\overline{L}_{obs}$ = average length of obstruction as described earlier in this chapter, in feet,

Q_{ob} = the discharge conveyed by the two overbank sections, in cfs, and

n_{ob} = the Manning n value for the overbanks, and

n_c = the Manning n value for the main channel.

In cases where the floodplain scale and discharge are significantly larger or smaller than those that were used in developing the regression formula, Equation 19 should not be used. The recommended approach for estimating the contraction ratio at this time is to compute a value from Equation 20 and check it against the values in Table 15:

$$CR = 1.4 - 0.333\left(\frac{F_{c3}}{F_{c4}}\right) + 1.86\left(\frac{Q_{ob}}{Q}\right)^2 - 0.19\left(\frac{n_{ob}}{n_c}\right)^{0.5} \qquad (20)$$

As with the expansion reach lengths, the modeler must use Equations 19 and 20 and the values from Table 15 with extreme caution when the prototype is outside of the range of data used in this study. The contraction ratio should not exceed 2.5:1 nor should it be less than 0.3:1.

9.2.3 Expansion Coefficients

The analysis of the data with regard to the expansion coefficients did not yield a regression equation which fit the data extremely well. Equation 21 was the best equation obtained for predicting the value of this coefficient:

$$C_e = -0.09 + 0.570\left(\frac{D_{ob}}{D_c}\right) + 0.075\left(\frac{F_{c2}}{F_{c1}}\right) \qquad (21)$$

In this equation

D_{ob} = hydraulic depth (flow area divided by top width) for the overbank at the fully-expanded flow section (Section 4), in feet, and

D_c = hydraulic depth for the main channel at the fully-expanded flow section, in feet.

It is recommended that the modeler use Equation 21 to find an initial value, then perform a sensitivity analysis using values of the coefficient that are 0.2 higher and 0.2 lower than the value from Equation 21. The plus or minus 0.2 range defines the 95% confidence band for Equation 21 as a predictor within the domain of the regression data. If the difference in results between the two ends of this range is substantial, then the conservative value should be used. The expansion coefficient should not be higher than 0.80.

9.2.4 Contraction Coefficients

The data of this study did not lend itself to regression of the contraction coefficient values. For nearly all of the cases the value that was determined was 0.1, which was considered to be the minimum acceptable value. The following table presents recommended ranges of the contraction coefficient for various degrees of constriction, for use in the absence of calibration information.

Table 16
Contraction Coefficient Values

Degree of Constriction	Recommended Contraction Coefficient
0% < b/B < 25%	0.3 - 0.5
25% < b/B < 50%	0.1 - 0.3
50% < b/B < 100%	0.1

The preceding recommendations represent a substantial improvement over the guidance information that was previously available on the evaluation of transition reach lengths and coefficients. They are based on data which, like all data, have a limited scope of direct application. Certain situations, such as highly skewed bridge crossings and bridges at locations of sharp curvature in the floodplain were not addressed by this study. Even so, these recommendations may be applicable to such situations if proper care is taken and good engineering judgment is employed.

Appendix A

References

Albertson, M.L., Y.B. Dai, R.A. Jensen, and H. Rouse, 1950, "Diffusion of Submerged Jets," *Transactions*, ASCE, Vol. 115, pp. 639-664.

Chow, V.T., 1959, *Open Channel Flow*, McGraw-Hill, New York.

DeVries, J.J., 1995, personal communication regarding undocumented flume studies performed in the early 1980's.

Federal Highway Administration, 1975, *Finite Element Model for Bridge Backwater Computation*, Report No. FHWA-RD 75-53, Washington, D.C.

Federal Highway Administration, 1978, *Hydraulics of Bridge Waterways*, Hydraulic Design Series No. 1, Washington, D.C.

Federal Highway Administration, 1986, *Bridge Waterways Analysis Model: Research Report*, Report No. FHWA-RD 86-108, McLean, Virginia.

Federal Highway Administration, 1991, *Stream Stability at Highway Structures*, Hydraulic Engineering Circular No. 20, McLean, Virginia.

Franques, J.T., and D.W. Yannitell, 1974, "Two-Dimensional Analysis of Backwater at Bridges," ASCE, *J. Hydraulics Division*, Vol. 100, March, pp. 379-392.

Golden Software, Inc., 1994, *Surfer for Windows: Contouring and 3D Surface Mapping, User's Manual*, Golden, CO.

Gray W.G., 1980, "Do Finite Element Models Simulate Surface Flow ?" *Third International Conference on Finite Elements in Water Resources*, S.Y. Wang et al., Eds., University of Mississippi, pp. 1.122-1.136.

Haan, C. T., 1977, *Statistical Methods in Hydrology*, Iowa State University Press, Ames Iowa, Chapter 10.

Hydrologic Engineering Center, 1990, *HEC-2 Water Surface Profiles User's Manual*, US Army Corps of Engineers, Davis, CA.

Hydrologic Engineering Center, 1995a, *UNET User 's Manual*, US Army Corps of Engineers, Davis, CA.

Hydrologic Engineering Center, 1995b, *HEC-RAS River Analysis System - User's Manual*, US Army Corps of Engineers, Davis, CA.

Hydrologic Engineering Center, 1995c, *HEC-RAS River Analysis System - Hydraulic Reference Manual*, US Army Corps of Engineers, Davis, CA.

Hydrologic Engineering Center, 1995d, *A Comparison of the One-Dimensional Bridge Hydraulic Routines from: HEC-RAS, HEC-2, and WSPRO*, US Army Corps of Engineers, Davis, CA.

Izzard, C.F., 1955, Discussion on "Backwater Effects of Open Channel Constrictions," by Tracy and Carter, *Transactions*, ASCE, Vol. 120, pp. 1008-1013.

King, I.P., 1994, *RMA-2V Two-Dimensional Finite Element Hydrodynamic Model*, Resource Management Associates, Lafayette, CA.

King, I.P., 1993, *RMA-10: A Finite Element Model for Three-Dimensional Density Stratified Flow*, New South Wales Environment Protection Authority, Bankstown, New South Wales, Australia.

Larock, B.E. 1995, Personal communication regarding WSPRO expansion loss formula.

Laursen, E.M., 1970, "Bridge Backwater in Wide Valleys," ASCE, *J. Hydraulics Division*, April, pp. 1019-1038.

Liu, H.K., J.N. Bradley, and E.J. Plate, 1957, *Backwater Effects of Piers and Abutments*, Colorado State University, Fort Collins, CO.

Norton, W.R., I.P. King, and G.T. Orlob, 1973, *A Finite Element Model for Lower Granite Reservoir*, Water Resources Engineers, Inc., Walnut Creek, CA.

STSC, Inc., 1991, *Statgraphics User Manual*, Rockville, MD.

Thompson, J.C., and W.P. James, 1988, "Two-Dimensional River Modeling of Buckhorn Creek," *Proceedings of the 1988 National Conference on Hydraulic Engineering*, ASCE, Colorado Springs, CO, pp. 1220-1225.

Tracy, H.J. and R.W. Carter, 1955, "Backwater Effects of Open Channel Constrictions," *Transactions*, ASCE, Vol. 120, pp. 993-1005.

United States Geological Survey, 1953, *Computation of Peak Discharge at Contractions*, USGS Circular No. 284.

United States Geological Survey, 1977, *Computation of Backwater and Discharge at Width Constrictions of Heavily Vegetated Flood Plains*, Water-Resources Investigation No. 76-129.

United States Geological Survey, 1978, *Backwater at Bridges and Densely Wooded Floodplains*, a series of Hydrologic Investigations Atlases, prepared in cooperation with the Federal Highway Administration and the State Highway Departments of Alabama, Louisiana, and Mississippi.

United States Geological Survey, 1979, *Backwater at Bridges and Densely Wooded Floodplains*, a series of Hydrologic Investigations Atlases, prepared in cooperation with the Federal Highway Administration and the State Highway Departments of Alabama, Louisiana, and Mississippi.

Walters, R.A. and R.T. Cheng, 1980, "Accuracy of an Estuarine Hydrodynamic Model Using Smooth Elements," *Water Resources Research*, Vol. 16, pp. 187-195.

Appendix B

Regression Equations in SI Units

Expansion Reach Length:

$$L_e = -90.9 + 78.3 \left(\frac{F_{c2}}{F_{c1}}\right) + 0.918\left(\overline{L}_{obs}\right) + 0.0515\left(Q\right) \tag{17B}$$

for which $\overline{R}^2 = 0.84$ and $S_e = 29.2$ meters, with

L_e = length of the expansion reach, in meters,

F_{c2} = main channel Froude number at Section 2,

F_{c1} = main channel Froude number at Section 1,

$\overline{L}_{obs}$ = average length of obstruction caused by the bridge approaches, in meters, and

Q = total discharge, m³/sec,

Expansion Ratio:

$$ER = \frac{L_e}{\overline{L}_{obs}} = 0.421 + 0.485\left(\frac{F_{c2}}{F_{c1}}\right) + 6.39 \times 10^{-4}\left(Q\right) \tag{18B}$$

for which $\overline{R}^2 = 0.71$ and $S_e = 0.26$.

Contraction Reach Length:

$$L_c = 80.2 + 11.8 \left(\frac{F_{c2}}{F_{c1}}\right) + 78.3 \left(\frac{Q_{ob}}{Q}\right)^2 - 17.9 \left(\frac{n_{ob}}{n_c}\right)^{0.5} + 0.161\left(\overline{L}_{obs}\right) \tag{19B}$$

with $\overline{R}^2 = 0.87$ and $S_e = 9.6$ meters. In this equation

Q_{ob} = the discharge conveyed by the two overbank sections, in m³/sec, and

n_{ob} = the Manning n value for the overbank sections.

71